Simulation and PC-based Implementation of a Vector Controlled Synchronous Motor Drive

A thesis submitted

in partial fulfillment of the requirements

for the degree of

MASTER OF TECHNOLOGY

by

R. Pavan Kumar Sukla

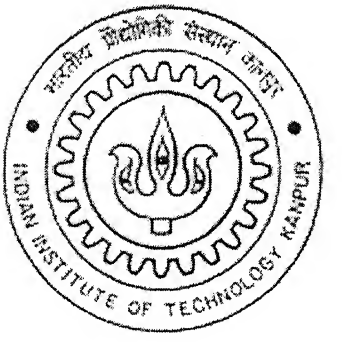

Department of Electrical Engineering
INDIAN INSTITUTE OF TECHNOLOGY, KANPUR
June 2005

To

my father

Sri R. Nageswara Rao

and

my mother

Smt. R.Padma Kumari

CERTIFICATE

This is certified that the work contained in this thesis entitled "**Simulation and PC–based Implementation of a Vector Controlled Synchronous Motor Drive**", by **R. Pavan Kumar Sukla,** has been carried out under my supervision and that this work has not been submitted elsewhere for any degree.

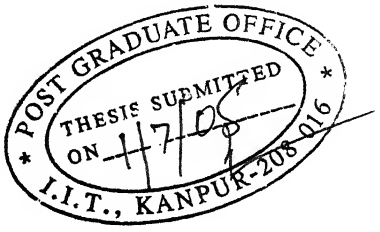

01/07/05

Dr. Shyama. P. Das

Associate Professor

Department of Electrical Engineering

Indian Institute of Technology

Kanpur, India

ACKNOWLEDGMENTS

I would like to acknowledge the contributions of many people who helped make this thesis possible.

I express my deep sense of gratitude and sincere thanks to my supervisor Dr. S. P. Das, for his invaluable guidance, inspiration, and constant encouragement throughout the course of this work. He explained the most complicated issues starting from the root of them. This helped me have a better understanding of the problem. Moreover, he has made me believe in myself. It has been a great experience to get the basic training of research under his rich experience and noble personality.

I want to express my sincere thanks to my teachers Dr. A. Ghosh, Dr. S. R. Doradla, Dr. P. Sensarma, Dr. L. Behera, Dr. N. Gupta and Dr. S. N. Singh whose courses have built the foundation upon which the work is based.

I take this opportunity to thank the research scholars Y. Y. Kolhatkar, Ranjan Kumar Behera, B. Kalyan Kumar and Meharegzi for their indebted support and continuous co-operation throughout this work.

I consider myself fortunate to have studied in IIT Kanpur. This place provided me an opportunity to learn a lot more than power electronics and drives. I also gratefully acknowledge the government of India for the financial assistance provided to me. I owe the completion of this work to my parents and my siblings who have continually offered encouragement and financial support throughout my academic career. It is because of their good wishes and encouragement I was able to cross several hurdles, which I faced throughout my academic career.

My stay at Hall-4 hostel will remain fresh and evergreen in my memory with the warmth and affection extended by my friends N. Kishore Kumar, V.L.N.S Sridhar Raja G. Naga Raju, Mr. & Mrs. Srinivas, R. Mahesh Kumar Reddy, T. Manoj, A. T. Rajesh.

I sincerely thank my classmates G. Srikanth, G. Kiran, E. Rammohan, M. Praveen, P. Hema Rani, K. N. Srinivas, D. D. Praveen Kumar, Bhaumik Sherdiwala, Navin Mohan Naidu, Prabodh Dewangan, Kingshuk, Sudipta, M. Rajender, K. Kiran and many others who made my stay at IIT a memorable thing in my life.

The thesis wouldn't have been completed without the active participation of our technical staff. I am very thankful to Mr. K. E. Hole of PCB Lab, Mr. Tiwari of electrical workshop, Mr. Amit Basu of power electronics lab. I thank Mr. D. D. Singh of stores for providing me with the hardware accessories for the project. I would like to thank Mr. J. S. Rawat and his colleagues of electrical department office for their support during my stay.

Finally, I would express my thanks to all those who have helped me directly or indirectly in the progress and completion of work.

R.Pavan Kumar Sukla

Abstract:

Vector control ensures good dynamic torque and speed response comparable to that of a separately excited dc motor drive. In the present thesis, the mathematical modeling and simulation of a vector controlled Synchronous Motor (SM) have been carried out. Hardware implementation of the Vector controlled drive is also done in the laboratory. An inverter, which is Current Regulated Pulse Width Modulated (CRPWM), is designed and fabricated. Hysteresis controller is used for current regulation. An algorithm based on vector control principle is developed for generating the reference phase currents of SM. The reference currents are compared with actual current values in the hysteresis controller and the output is used to drive the inverter. The field current is kept constant. An incremental encoder with 2500 pulses per revolution is used to estimate the rotor position accurately in the presence of multiple direction reversals. The drive system was tested for different test conditions and results were found to be satisfactory.

Keywords: Synchronous Motor, Vector Control, CRPWM, hysteresis controller, PC–based implementation, incremental encoder.

Contents

List of Figures

List of Symbols

ρ_{dg} , ρ_{qg}	permeance in direct and quadrature axis respectively.
L_{aa} , L_{bb}, L_{cc}	self inductances of phase A, B, C respectively.
L_{al}, L_{bl}, L_{cl}	leakage inductance of phase A, B, C respectively.
L_{fd}	Field self inductance.
L_{lfd}	Field leakage inductance.
L_{lkd}	d-axis damper leakage inductance.
L_{lkq}	q-axis damper leakage inductance.
L_{kd}	d-axis damper self inductance.
L_{kq}	q-axis damper self inductance.
L_{af}, L_{bf}, L_{cf}	inductance between phase A, B, C and field respectively.
L_{ab}	mutual inductance between A and B phase.
L_{bc}	mutual inductance between B and C phase.
L_{ca}	mutual inductance between C and A phase.
L_{ag}	self inductance of phase A due to air gap flux.
$L_{as,kd}$	inductance between phase A and d-axis damper winding.
$L_{bs,kd}$	inductance between phase B and d-axis damper winding.
$L_{cs,kd}$	inductance between phase A and d-axis damper winding.
$L_{as,kq}$	inductance between phase A and q-axis damper winding.
$L_{bs,kq}$	inductance between phase A and q-axis damper winding.
$L_{cs,kq}$	inductance between phase A and q-axis damper winding.
Ψ_{ag}	air gap flux.
Ψ_{abcs}	Flux matrix in phase format.

$\psi_{d,q,0}$	Flux matrix in d-q form.
ψ_s	Stator flux linkage.
ψ_f	Field flux linkage.
Ψ_g	Air gap flux linkage.
Ψ_{ds}	d-axis stator flux linkage.
Ψ_{qs}	q-axis stator flux linkage.
Ψ_{kd}	d-axis damper flux linkage.
Ψ_{kq}	q-axis damper flux linkage.
i_a, i_b, i_c	Stator phase currents.
i_f	field current.
i_{abcs}	stator current matrix in phase format.
$i_{d, q, 0}$	stator current matrix in d-q form.
$i_{f, kd, kq}$	rotor current matrix.
V_{abc}	voltage equation in phase format.
$V_{d,q,0}$	voltage matrix in d-q format.
V_{ds}, V_{qs}	d-axis and q-axis voltages.
r_s	armature resistance per phase.
r_f	field resistance.
r_{kd}, r_{kq}	d-axis and q-axis damper resistance.
N_a	effective number of per-phase turns.
θ_r	rotor electrical angle.

T_{em}	Electromagnetic torque.
T_L	Load torque.
δ	Torque angle (angle between field axis and stator flux vector).
w_b	Base speed in electrical rad/s.
ω_r	rotor speed in electrical rad/s.
p	time derivative operator.
P	number of poles.
J	polar moment of inertia.
h	Hysteresis band.
f	frequency in cycles/s.
I_T^*	reference torque component of stator current.
I_M^*	reference magnetizing current.

Chapter - 1

Introduction

1.1 General

The idea of vector controlled AC motor drives is based on the excellent control properties of DC motors, where torque and motor magnetic flux can be independently controlled. In the development of vector controlled AC motor technology, the first theoretical problem was to model a three phase AC coil system in a way that separation between torque and flux control could be done.

Extensive research work of synchronous machine theory was done in the 1920s mainly in the United States. Motivation for synchronous motor modeling at that time was not vector control development, but the increasing importance of synchronous machines in power systems. Improved models for synchronous machines were required, particularly for the analysis of abnormal situations in power networks. One of the most thorough researches on synchronous machine theory has been done by R. E. Doherty and C. A. Nickle [1], who represented their results in a four paper series at the end of 1920s (Doherty & Nickle 1926, 1927, 1928 and 1930 [1]). These papers already included the two-axis modeling of synchronous machine. The more detailed mathematical analysis of the two-axis model was presented by Park (1929) [2]. Park's two axis mathematical analysis was a success, and that is the reason why the synchronous motor two-axis model carries his name. Park's two-axis model includes direct and quadrature axes representation where the actual measurable phase quantities were replaced by calculatory elements in **rotor** reference frame for a synchronous machine.

The next major steps in AC machine modeling were taken in the 1950s, when the space vector theory was developed for multi-phase AC machines in Hungary. The space vector theory made it possible to combine motor phase quantities into a single complex vector variable in any reference frame. This was a breakthrough, which made the final vector control innovation possible. An important factor, which made controlled electrical drives more interesting on a practical level, was the intensive development of semiconductor devices in the middle of this century. The first breakthrough was the development of the transistor in 1948. The introduction of the first commercial thyristor ten years later was the second discovery. This thyristor was the first controllable semiconductor power switch, which made the true electronic control of power electric circuits possible. In the 1960s, the new semiconductor technology was intensively applied in controlled DC motor drives, and Thyristor Bridge supplied drives gained popularity in industrial and traction applications.

At the same time, intensive research work has been done to develop AC drive systems with variable frequency. The first variable frequency AC drives were based on the pulse width modulation (PWM), (Stemmler 1994). At the end of 1960s, German engineer Felix Blaschke [3] made an innovation, which lead to the development of the first field oriented **vector controlled** AC motor drive. He represented the principle of field orientation and the separate control of motor magnetic flux linkage and torque, the so called transvector control, (Blaschke 1972) [3]. This method made it possible for the first time to control AC motors like DC motors.

Transvector control for large **synchronous motors (SM's)** was introduced by Bayer et al. 1971[4]. At the same time, intensive research work was going on in the Finnish company Stromberg to develop the asynchronous motor speed control. Asynchronous motors were one of the company's main products, and they suited very well for traction drives and industrial applications due to their robustness and competitive price. The solution was not a vector control, but a PWM based variable frequency control, which was named scalar control. The main designer of the new technology was Finnish engineer Martti Harmoinen. As a result, the first worldwide AC motor traction drive was introduced in the underground of Helsinki at the beginning of 1980s. Another important application area, where Stromberg used for the first time worldwide AC motor technology, was the sector of the paper machine speed controlled drives. In 1980s, AC motor drive technology was getting more popular in the different application areas. Because of the growing demand for high dynamic performance the Blaschke's idea of field oriented vector control was introduced into the field of asynchronous machines as well. During the whole decade the vector controlled asynchronous motor has been an object for intensive research work as well as product development. The wide survey of the vector control methods for AC drive systems has been represented by Leonhard (1996) [5] and Vas (1990) [6].

Vector control, also described as field oriented control, is being increasingly used for speed control of AC motors. This is because, with vector control, it is possible to achieve high dynamic performance, equaling that of the separately excited DC motor, in variable speed AC drives. Therefore, vector control makes it possible to use, in place of a DC motor, an AC motor, which is more rugged and does not have the commutator or

other rubbing contacts, and is therefore free of associated maintenance requirements and sparking problems.

1.2 Objectives of Thesis

The present thesis, which aims at the design and development of a Vector Controlled synchronous motor drive system, fulfils the following objectives.

- A comprehensive digital computer simulation of Vector controlled SM drive system in Park Reference frame [7].
- Design and fabrication of 3-phase inverter.
- Design and fabrication of 3-phase Hysteresis controller.
- A PC-based implementation and development of controller for drive.

1.3 Scope of the Thesis

The work presented in the thesis is organised in four chapters.

Chapter-1 gives a brief historical review about vector control principle and synchronous motor vector control. It also outlines the basic objectives of the thesis.

Chapter-2 describes, at length, d-q theory of synchronous machine. Mathematical modeling of vector controlled synchronous motor is carried out. Digital models for synchronous motor, 3-phase inverter and hysteresis controller are developed. Simulation of this whole system is carried out using Simulink, Matlab 6.5. Plots of speed, torque, power factor, currents, etc are presented in this chapter.

Chapter-3 gives details of the practical implementation of vector controlled synchronous motor. It also outlines the design and fabrication of 3-phase inverter, hysteresis controller. A hybrid controller for drive system is developed. The digital controller part

involves a Pentium-III PC housed with necessary data acquisition and timer cards. A high resolution incremental encoder is used to calculate speed and rotor position. The algorithm is developed on vector control principle of SM and the programming is done in C-language. Experimental results and algorithm are also presented in this chapter.

Chapter-4 is the concluding chapter, which highlights the main contributions of the thesis and enumerates the scope for further research in this area.

Chapter 2

Modeling and Simulation of a Vector Controlled SM Drive System

2.1 Introduction

Initially, the present chapter deals with the different aspects of controlling a Synchronous Motor (SM). Later on it deals with d-q theory of synchronous machine. Mathematical modeling of vector controlled SM is carried out. Digital models for the synchronous motor, 3-phase inverter, hysteresis controller are developed. Simulation of Vector controlled SM drive system is carried out for different conditions and results were plotted.

2.2 Scalar control

The control of SM is categorized into two groups: scalar and vector control. Different types of scalar control are discussed in this section. A synchronous machine drive system has essentially two different modes of operation. One is the open-loop true synchronous motor mode, where the machine speed is controlled by an independent oscillator. The other is known as a self–control mode, where the variable–frequency inverter (or cycloconverter) control pulses are derived from the rotor position sensor. In the latter mode, the supply frequency is no longer independent but is linked with rotor speed, which may vary with variation of load torque.

2.2.1 Open loop Volts/Hertz control

An example of independent frequency control is the open loop volts/hertz control shown in Fig. 2.1.This method of speed control is very popular in multiple reluctance or

permanent machine drives, where close speed tracking is essential in such applications as fiber–spinning mill. Here the machine is supplied by an inverter and the machine speed is uniquely related to the command frequency ω_e^*. Maintaining a constant volts/hertz ratio makes the air gap flux constant, permitting maximum torque availability of the machine. At a certain frequency and voltage condition, if the load torque increases, the developed torque increases to match it, until the stability limit is reached. The speed can be varied from zero to the full value by gradually varying the frequency. Beyond the base speed, the dc link voltage saturates and the machine enters into the field weakening or constant – power region, where the torque decreases with an increase in frequency. The air gap flux can be independently controlled by a closed loop, if desired.

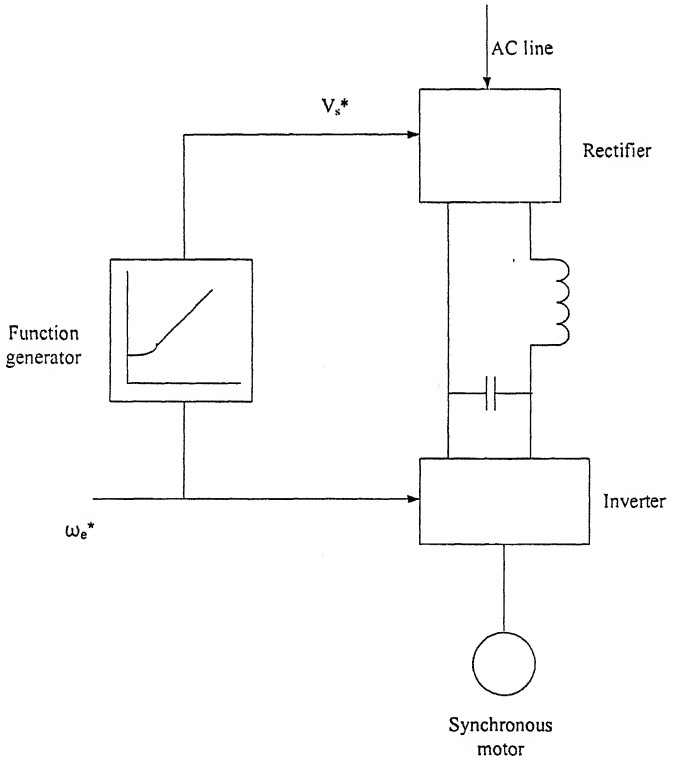

Fig. 2.1 Open loop Volts/Hertz control of a synchronous motor.

2.2.2 Self –control mode

The self control of synchronous motor with electronic devices is as old as the "Thyratron motor" reported by Alexanderson and Mittag in 1934[8]. Further significant development in this area had to wait until the availability of thyristor in the market in early 1960's. Since then a number of publications have reported the development of SCSM drives employing dc link inverter [9-13] and cycloconverter [14]. An attempt is made in this section to set forth the basic principles of a SCSM drive emphasizing its close similarity to a dc motor drive. A synchronous machine (Fig. 2.2) operating in the self-control mode can be defined as an electronically commutated motor, brushless dc motor or commutatorless-brushless motor. The reason for this definition is that in this mode of operation, the synchronous machine is analogous to a dc machine in the following way. Internally, a dc machine can be viewed as a synchronous machine in which the field is stationary but the armature with multiphase ac winding is rotating. The ac supply to the armature is derived from the input dc supply through commutators and brushes, which can be viewed as a mechanical shaft position-sensitive inverter. A synchronous machine in the self-control mode is somewhat analogous, but here the field is rotating and the armature is stationary, and it is supplied by a shaft–position-controlled electronic inverter. The advantages of replacement of mechanical commutators and brushes in a dc machine by electronic commutation are obvious. Self-control modes of a synchronous machine may be valid whether by a voltage–fed inverter, a current fed-inverter, or a cycloconverter. The self-controlled synchronous machine has the advantages that it cannot fall out of step by the steady-state stability limit and rarely shows any transient stability problem.

The self control principle is illustrated in Fig. 2.2 by a current fed inverter. The machine rotor has a shaft position sensor and the sensor signal is processed through a delay angle control circuit to generate the inverter firing pulses as shown. This self-control mode relates the inverter frequency uniquely with machine speed.

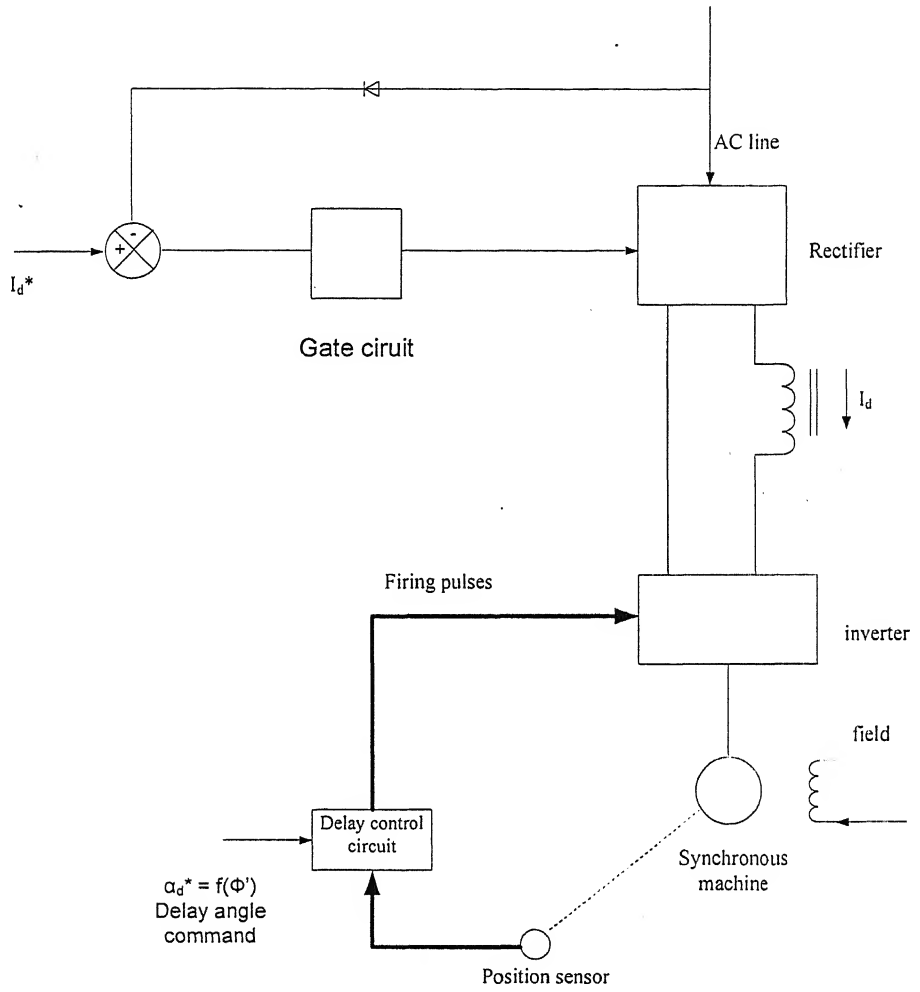

Fig. 2.2 Synchronous motor self-control principle.

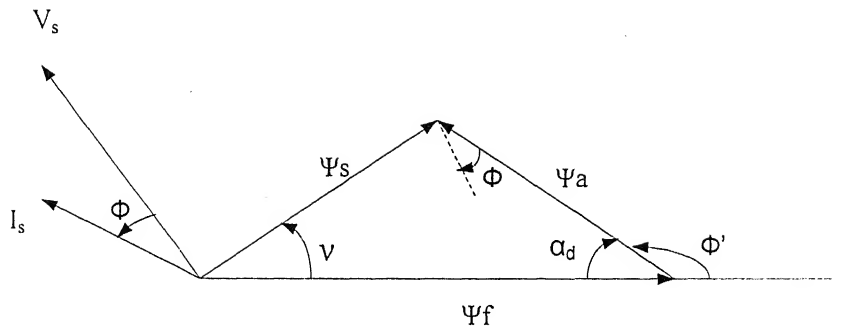

Fig. 2.3 Phasor diagram of synchronous machine at leading pf.

Figure 2.3 shows the fundamental–frequency phasor diagram for load commutation of the inverter where the stator current I_s leads the stator voltage V_s by the angle Φ. The field flux ψ_f, which is related to the rotor position, is established independently by the field current. The magnitude of the stator current controlled by the rectifier determines the magnitude of the armature reaction flux $\psi_a = I_s L_s$, and the phasor can be positioned at a desirable angle by the firing angle α_d. In the Fig. 2.3, the phasor ψ_a leads ψ_f by the angle Φ' so that the resultant stator flux ψ_s (including leakage) induces the stator voltage V_s, which lags the stator current I_s by an angle Φ. The angle Φ' can be given as

$$\Phi' = 180° - \alpha_d = \nu + 90° + \Phi \qquad (2.1)$$

where ν is the angle of the ψ_s phasor. The magnitudes of I_s, Φ', and I_f can be controlled with speed to establish the optimum commutation condition.

2.2.3 Review of DC motor

Before proceeding with the development of the principles of vector control and field orientation, a brief review of torque control in dc machines is presented. The basic structure

is schematically illustrated in Fig. 2.4 along with the resulting orientation of the armature MMF and the field flux. The action of commutator is to reverse the direction of armature winding currents as the coils pass the brush position such that armature current distribution is fixed in space no matter what rotor speed exists. As shown in Fig. 2.4, the field flux and armature MMF are maintained in a mutually perpendicular orientation independent of rotor speed. The result of this orthogonality is that the field flux is unaffected by the armature current except for second order, nonlinear effects.

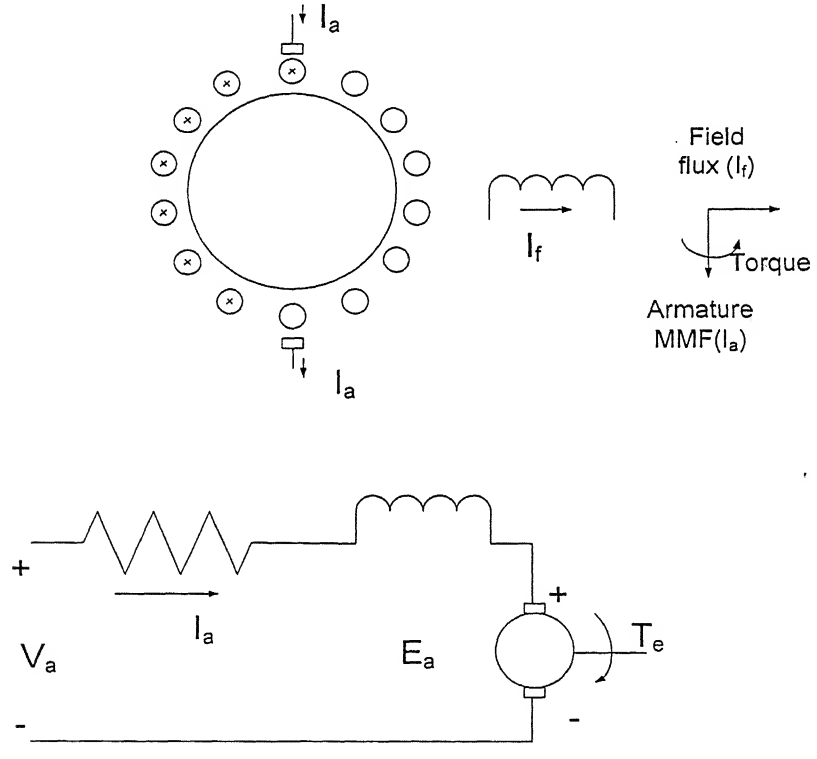

Fig. 2.4 Torque development in a dc motor.

The electromagnetic interaction between the field flux and the armature MMF results in two basic outputs: an induced voltage proportional to rotor speed,

$$E_a = \frac{P}{2} \lambda_{af} \omega_{rm} \qquad (2.2)$$

and an electromagnetic torque proportional to armature current

$$T_e = \frac{P}{2}\lambda_{af} I_a = \frac{P}{2}\frac{L_{af}}{L_f}\lambda_f I_a \qquad (2.3)$$

where ω_{rm} is the rotor speed in mechanical radians per second.

P is the number of poles, λ_{af} is the flux produced by the field current which links the armature winding and L_{af}, L_f are mutual inductance between field and armature winding and the field self inductance respectively.

It is important to note that the simplicity of the model is strongly dependent on the mutually perpendicular orientation of the flux and MMF. If this orthogonality were disturbed two major complications occur:

1. The field flux is no longer dependent of the armature current since there will be an armature MMF component in field axis
2. The voltage and torque equations (2.2 and 2.3) will be modified by addition of an angle dependent function (sine of angle between axes).

As expressed in equation 2.3, with a constant value of field flux, the torque is directly proportional to armature current. Thus, the torque can be adjusted as accurately and as rapidly as the armature current can be adjusted and controlled.

So the requirements in a dc machine for torque control are:

1. An independently controlled armature current to overcome the effects of armature winding resistance, leakage inductance and induced voltage.
2. An independently controlled or constant value of the field flux.

3. An independently controlled orthogonal spatial angle between the field flux axis and the armature MMF axis to avoid interaction of the armature MMF and the field flux.

If all three of these requirements are met at every instant of time, the torque will instantaneously follow the current and instantaneous torque control will result. If, as occurring in certain systems, these requirements are only met for steady state conditions, only steady state torque control will result. During the transient period, the torque will not follow the current exactly and this may or may not be satisfactory for many industrial applications.

In dc machine, requirements 2 and 3 are assured by the commutator and the separate field excitation system (dc winding or permanent magnet). In ac machines, these requirements must be achieved by external controls and thus the situation is more complex and somewhat more difficult to understand.

2.3 D-Q theory of Synchronous machine

In this section a d-q model for synchronous motor has been described .The development of an equivalent circuit for the synchronous machine operating under balanced sinusoidal steady conditions is considered. Phasor diagrams have been drawn to clarify the confusions that exist with regard to conventions.

An SM has three windings on the stator and a field winding and a short circuited damper winding on the rotor. Each of these windings also has a magnetic coupling with every other winding i.e. it has a mutual inductance associated with it and with every other winding. The damper windings consist of a large number of copper bars which are shorted by end rings. As with any modeling, certain assumptions are made:

1. Effect of saturation of the magnetic circuit is ignored i.e. the magnetic circuit is considered to be linear.
2. Hysteresis and eddy current losses are neglected.
3. Space MMF and flux distribution are assumed to be sinusoidal.
4. The effect of the stator slots is not considered.
5. The damper windings assumed to be two independent windings: one along the rotor direct axis and the other one along the quadrature axis.

Since the air gap of a salient pole synchronous machine varies along the inner circumference of the stator, the machine is no longer symmetrical in the sense of an induction motor. Referring to Fig. 2.5 it is clear the self inductance of any armature winding will pulsate once each time the rotor moves one pole pitch.

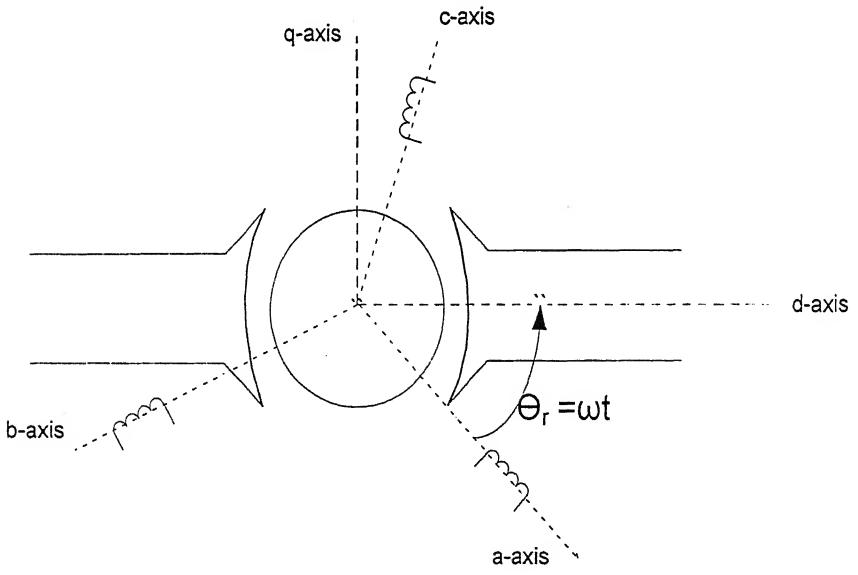

Fig. 2.5 Basic two pole synchronous machine.

Expressions for the various inductances in terms of rotor position angle (θ_r) can be shown as follows [15].

Armature self inductances.

Armature self inductance of phase A is given by

$$L_{aa} = L_{al} + L_{ag}$$

$$L_{ag} = \frac{\psi_{ag}}{i_a} = N_a^2(\rho_{g0} + \rho_{g2}\cos(2\theta_r)$$

$$= L_{g0} + L_{g2}\cos 2\theta_r \qquad (2.4)$$

where $\rho_{g0} = (\rho_{dg} + \rho_{qg})/2$, $\rho_{g2} = (\rho_{dg} - \rho_{qg})/2$

Therefore

$$L_{aa} = L_{al} + L_{g0} + L_{g2}\cos 2\theta_r \qquad \text{and similarly}$$

$$L_{bb} = L_{bl} + L_{g0} + L_{g2}\cos 2(\theta_r - 120°)$$

$$L_{cc} = L_{cl} + L_{g0} + L_{g2}\cos 2(\theta_r + 120°) \qquad (2.5)$$

Armature Mutual Inductances:

$$L_{ab} = L_{ba} = -\frac{L_{g0}}{2} + L_{g2}\cos(2\theta_r - 120°)$$

$$L_{bc} = L_{cn} = -\frac{L_{g0}}{2} + L_{g2}\cos 2\theta_r \qquad (2.6)$$

$$L_{ca} = L_{ac} = -\frac{L_{g0}}{2} + L_{g2}\cos(2\theta_r + 120°)$$

Inductance between stator and rotor;

$$L_{af} = L_{md}\cos\theta_r$$

$$L_{bf} = L_{md}\cos(\theta_r - 120°) \qquad (2.7)$$

$$L_{cf} = L_{md}\cos(\theta_r + 120°)$$

where L_{md} is mutual inductance between phase A and field winding when they are aligned.

Inductance between stator and d-axis damper winding

$$L_{as,kd} = L_{md} \cos \theta_r$$
$$L_{bs,kd} = L_{md} \cos(\theta_r - 120°) \quad (2.8)$$
$$L_{cs,kd} = L_{md} \cos(\theta_r + 120°)$$

Inductance between stator and q-axis damper winding

$$L_{as,kq} = -L_{mq} \sin \theta_r$$
$$L_{bs,kq} = -L_{mq} \sin(\theta_r - 120°) \quad (2.9)$$
$$L_{cs,kq} = -L_{mq} \sin(\theta_r + 120°)$$

Therefore the inductance matrix of stator, L_{abc}, can be written as

$$L_{abc} = \begin{bmatrix} L_{aa} & L_{ab} & L_{ac} \\ L_{ba} & L_{bb} & L_{bc} \\ L_{ca} & L_{cb} & L_{cc} \end{bmatrix} \quad (2.10)$$

Similarly the inductance matrix, L_{sr}, between stator and rotor is

$$L_{sr} = \begin{bmatrix} L_{md}\cos\theta_r & L_{md}\cos\theta_r & -L_{mq}\sin\theta_r \\ L_{md}\cos(\theta_r - 120°) & L_{md}\cos(\theta_r - 120°) & -L_{mq}\sin(\theta_r - 120°) \\ L_{md}\cos(\theta_r + 120°) & L_{md}\cos(\theta_r + 120°) & -L_{mq}\sin(\theta_r + 120°) \end{bmatrix} \quad (2.11)$$

The flux equation in matrix form can be written as

$$\psi_{abcs} = [L_{abcs}]\, i_{abcs} + [L_{sr}]\, i_{f,kd,kq} \quad (2.12)$$

Flux equation in d-q form can be obtained using transformation matrix C and equation 2.12

$$C\psi_{abcs} = C\,[L_{abcs}]\, i_{abcs} + C\,[L_{sr}]\, i_{f,kd,kq}$$
$$\psi_{d,q,0} = C\,[L_{abcs}]\, C^{-1}\, i_{d,q,0} + C\,[L_{sr}]\, i_{f,kd,kq}$$
$$= [L_{d,q,0}]\, i_{d,q,0} + C\,[L_{sr}]\, i_{f,kd,kq} \quad (2.13)$$

where $C = \frac{2}{3}\begin{bmatrix} \cos\theta_r & \cos(\theta_r - 120) & \cos(\theta_r + 120) \\ -\sin\theta_r & -\sin(\theta_r - 120) & -\sin(\theta_r + 120) \\ \frac{1}{2} & \frac{1}{2} & \frac{1}{2} \end{bmatrix}$ is transformation matrix in

Park's reference frame and

$$C[L_{sr}] = \frac{2}{3}\begin{bmatrix} \cos\theta_r & \cos(\theta_r - 120) & \cos(\theta_r + 120) \\ -\sin\theta_r & -\sin(\theta_r - 120) & -\sin(\theta_r + 120) \\ \frac{1}{2} & \frac{1}{2} & \frac{1}{2} \end{bmatrix} \begin{bmatrix} L_{md}\cos\theta_r & L_{md}\cos\theta_r & -L_{mq}\sin\theta_r \\ L_{md}\cos(\theta_r - 120) & L_{md}\cos(\theta_r - 120) & -L_{mq}\sin(\theta_r - 120) \\ L_{md}\cos(\theta_r + 120) & L_{md}\cos(\theta_r + 120) & -L_{mq}\sin(\theta_r + 120) \end{bmatrix}$$

$$= \begin{bmatrix} L_{md} & L_{md} & 0 \\ 0 & 0 & L_{mq} \\ 0 & 0 & 0 \end{bmatrix}$$

The fundamental equation of voltage of a synchronous motor is

$$V_{abc} = r_s\, i_{abcs} + p\,\psi_{abcs} \qquad (2.14)$$

Equation 2.14 can be transformed by Park's transformation to get d-q form

$$C\ V_{abc} = C\ r_s\, i_{abcs} + C\ p\,\psi_{abcs}$$

resulting in

$$V_{dq0} = r_s\, i_{dq0} + p\,(C\,\psi_{abc}) - (p\,C)\,\psi_{abc} \qquad (2.15)$$

where $(p\,C)\,\psi_{abc} = \begin{bmatrix} \psi_{qs} \\ -\psi_{ds} \\ 0 \end{bmatrix} p\,\theta_r$

Equation 2.15 can be written in expanded form as

$$\begin{aligned} V_{ds} &= r_s i_{ds} + p\,\psi_{ds} - \omega_r \psi_{qs} \\ V_{qs} &= r_s i_{qs} + p\,\psi_{qs} + \omega_r \psi_{ds} \\ V_f &= r_f i_f + p\,\psi_f \\ V_{kd} &= r_{kd}\, i_{kd} + p\,\psi_{kd} \\ V_{kq} &= r_{kq}\, i_{kq} + p\,\psi_{kq} \end{aligned} \qquad (2.16)$$

where flux terms are given by

$$\begin{aligned}
\psi_{ds} &= L_{ds} i_{ds} + L_{md} i_f + L_{md} i_{kd} . \\
\psi_{qs} &= L_{qs} i_{qs} + L_{mq} i_{kq} . \\
\psi_f &= L_f i_f + L_{md} i_{kd} + L_{md} i_{ds} . \\
\psi_{kd} &= L_{kd} i_{kd} + L_{md} i_f + L_{md} i_{ds} . \\
\psi_{kq} &= L_{kq} i_{kq} + L_{mq} i_{qs} .
\end{aligned} \tag{2.17}$$

So from equations 2.17 and 2.18, we get

$$\begin{aligned}
V_{ds} &= r_s.i_{ds} + L_{ds}.p.i_{ds} + L_{md}.p.i_f - w_r.L_{qs}.i_{qs} - w_r.L_{qs}.i_{qs} - w_r.L_{mq}.i_{kq} + L_{md}.p.i_{kd}. \\
V_{qs} &= r_s.i_{qs} + L_{qs}.p.i_{qs} + L_{md}.p.i_{kq} + w_r.L_{ds}.i_{ds} + w_r.L_{md}.i_f + w_r.L_{md}.i_{kd} \\
V_f &= r_f i_f + L_f p i_f + L_{md} p i_{ds} + L_{md} p i_{kd} \\
V_{kd} &= r_{kd} i_{kd} + L_{kd} p i_{kd} + L_{md} p i_f + L_{md} p i_{ds} \\
V_{kq} &= r_{kq} i_{kq} + L_{kq} p i_{kq} + L_{mq} p i_{qs}
\end{aligned} \tag{2.18}$$

Equation (2.18) can be expressed in matrix form as

$$\begin{bmatrix} V_{ds} \\ V_{qs} \\ V_f \\ V_{kd} \\ V_{kq} \end{bmatrix} = \begin{bmatrix} r_s & -w_r L_{qs} & 0 & 0 & -w_r L_{mq} \\ w_r L_{ds} & r_s & w_r L_{md} & w_r L_{md} & 0 \\ 0 & 0 & r_f & 0 & 0 \\ 0 & 0 & 0 & r_{kd} & 0 \\ 0 & 0 & 0 & 0 & r_{kq} \end{bmatrix} \begin{bmatrix} i_{ds} \\ i_{qs} \\ i_f \\ i_{kd} \\ i_{kq} \end{bmatrix} + \begin{bmatrix} L_{ds} & 0 & L_{md} & L_{md} & 0 \\ 0 & L_{qs} & 0 & 0 & L_{mq} \\ L_{md} & 0 & L_f & L_{md} & 0 \\ L_{md} & 0 & L_{md} & L_{kd} & 0 \\ 0 & L_{mq} & 0 & 0 & L_{kq} \end{bmatrix} \begin{bmatrix} i_{ds} \\ i_{qs} \\ i_f \\ i_{kd} \\ i_{kq} \end{bmatrix} \tag{2.19}$$

equivalent circuit of a salient pole synchronous machine in the Park reference frame

vn in Fig. 2.6 [7]

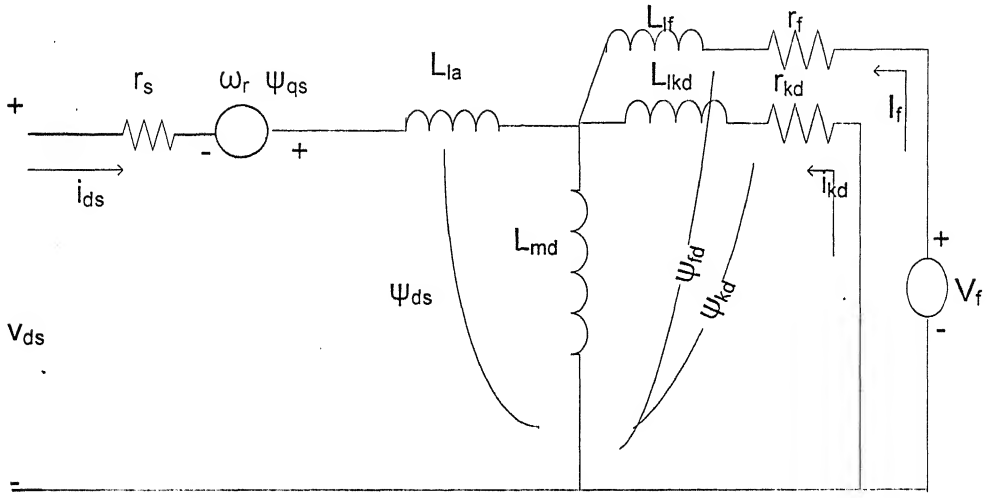

d-axis circuit

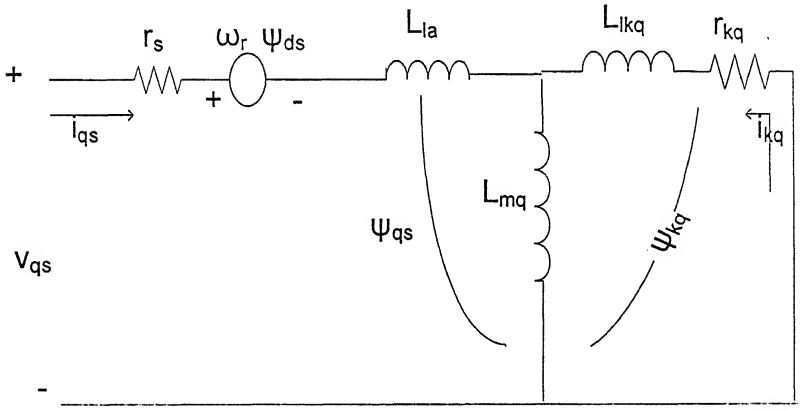

q- axis circuit

Fig. 2.6 Equivalent circuit of the SM in the Park reference frame.

2.7 are d, q diagrams representing constant d, q quantities in two axes, i.e., the

plex vector interpretation of the scalar d-q axis quantities.

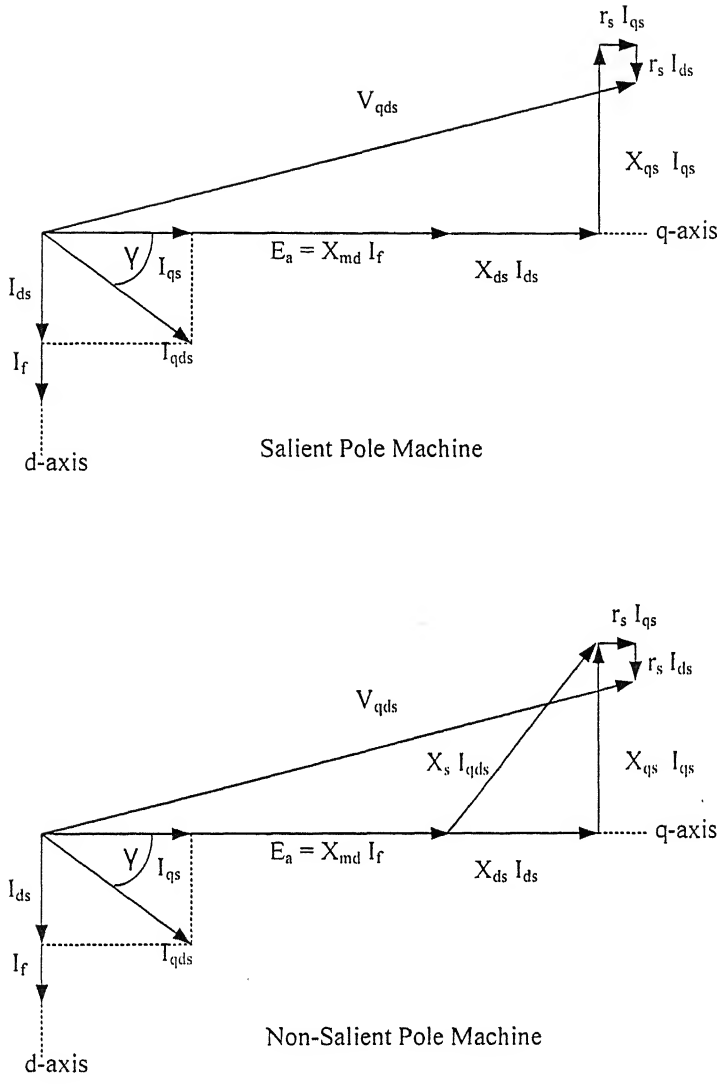

Fig. 2.7 Vector diagram of SM in d-q co-ordinates.

e torque can be given by

$$= \frac{3}{2}\frac{P}{2}[(L_{ds} - L_{qs})i_{ds}i_{qs} + L_{md}i_f i_{qs} + L_{md}i_{kd}i_{qs} - L_{mq}i_{kq}i_{ds}] \tag{2.20}$$

e torque can be rewritten in terms of angle γ

$$\text{action torque} = \frac{3}{2}\frac{P}{2}\frac{1}{w_b}E_a I_{qds}\cos\gamma \tag{2.21a}$$

$$\text{Reluctance torque} = = \frac{3}{2}\frac{P}{2}\frac{1}{w_b}(X_{ds} - X_{qs})I_{qds}^2 \cos\gamma \sin\gamma \qquad (2.21b)$$

Equations 2.19 and 2.20 along with the 2.22 & 2.23 are the basic equations of synchronous motor.

The electromagnetic torque equation is

$$T_{em} = \frac{P}{2} J \frac{d\omega_r}{dt} + \frac{P}{2} B\omega_r + T_L \qquad (2.22)$$

where $\frac{d\theta_r}{dt} = \omega_r$ (2.23)

is rotor speed in electrical rad/s.

2.4 Vector control

The concept of rotor position feedback and vector control of machine stator current to maintain the space angle between the field winding and stator MMF results in stator currents which translate to controlled values of i_{qs} and i_{ds} in the rotor reference frame. This is a result of the instantaneous control of the phase of the stator current to always maintain the same orientation of the stator MMF vector relative to the field winding in the d-axis of the d, q model. The resulting axis currents are illustrated in Fig. 2.8

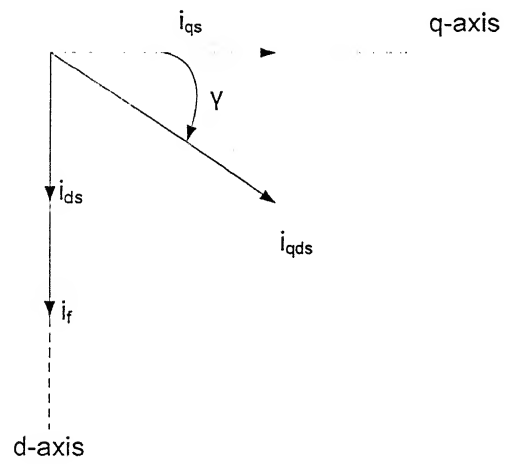

Fig. 2.8 Synchronous machine currents in d, q axes.

The concept of **vector control (or field orientation)** is that the electrical space angle between the stator current and field mmf is always maintained at 90^0. This means $\gamma = 0$ (Fig. 2.8) or $i_{ds} = 0$.

2.4.1 Dynamics of Synchronous machine field orientation

The dynamics of field orientation case ($\gamma = 0$) is simple with the assumptions:

1. The stator current is the independently controlled input variable, and
2. The orientation of the stator d, q currents is maintained for all speeds including transient changes.

With $\gamma = 0$, there is only a q-axis stator current component, i.e. $i_{ds} = 0$ for all transient conditions. Under these conditions the rotor voltage equations and flux linkage relations reduce to:

d-axis damper circuit:

$$V_{kd} = r_{kd} i_{kd} + L_{kd} p i_{kd} + L_{md} p i_f = 0 \tag{2.24}$$

q-axis damper circuit:

$$V_{kq} = r_{kq} i_{kq} + L_{kq} p i_{kq} + L_{mq} p i_{qs} = 0 \tag{2.25}$$

Field circuit

$$V_f = r_f i_f + L_{md} p i_{kd} + L_f p i_f \tag{2.26}$$

And the torque expression (2.20) reduces to

$$T_{em} = \frac{3}{2}\frac{P}{2} L_{md} (i_f + i_{kd}) i_{qs} \tag{2.27}$$

This special case is illustrated in Fig. 2.9 where the stator current is all in the q-axis (γ=0). For this situation the field current in d-axis and the stator current in q-axis are 90°

apart as is the case in the dc machine. Because of absence of d-axis stator current there is no reluctance torque and only the q-axis reactance is involved in finding the terminal voltage, i.e., there is no direct magnetization or demagnetization of the d-axis. The field winding acts to produce flux in the d-axis.

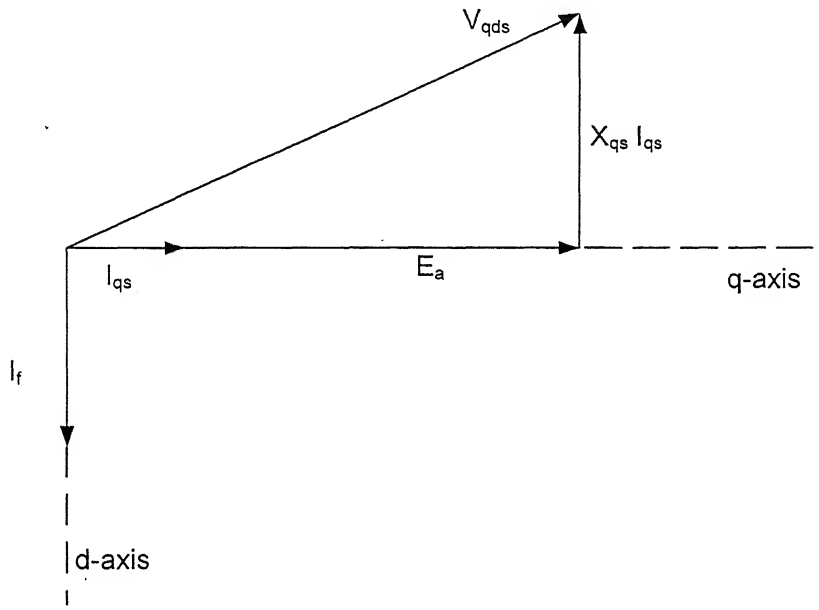

Fig. 2.9 Vector diagram for the field orientation.

2.4.2. Constant Field current operation (Constant torque Region)

With a fixed dc voltage applied to the field winding, solution of the above equations is

$$i_{kd} = 0.\ and$$

$$i_f = \frac{V_f}{r_f} = I_f \qquad (2.28)$$

This is the same as for steady state conditions and is a direct result of the absence of any d-axis stator current. The d-damper circuit and field circuit is a pair of coupled coils in

the d-axis without any interaction with the stator as a result of the "field orientation". There is complete "decoupling" of the d-axis from the stator windings. The q-axis equations can be combined and written in a form to emphasize i_{qs} as an input quantity to yield

$$r_{kq} i_{kq} + pL_{kq} ikq = -pL_{mq}\, i_{qs} \tag{2.29}$$

And solving for i_{kq}

$$i_{kq} = -\frac{L_{mq} p}{r_{kq} + L_{kq} p} i_{qs} \tag{2.30}$$

Thus, a change in i_{qs} will induce a transient q-axis damper current, which will have an initial value of

$$\Delta i_{kq}(0) = -\frac{L_{mq}}{L_{kq}} \Delta i_{qs}(0) \tag{2.31}$$

Where Δi_{qs} is the change in i_{qs}. This transient q-axis damper will decay with self-time constant (open circuit time constant) of the damper, L_{kq}/r_{kq}. There will, however, be no torque produced by this transient q-axis damper current because there is no d-axis stator current.

The torque for the case of constant field excitation is

$$T_e = \frac{3}{2}\frac{P}{2} L_{md} I_f i_{qs} \tag{2.32}$$

a result identical to steady state (since $L_{md} I_f = E/\omega_r$). Thus, the torque response for field orientation is instantaneous and follows the commanded value of i_{qs} exactly.

.3 Variable Field Excitation (Field Weakening Region)

he field current is changed, there will be an induced d-axis damper current, which can evaluated by solving field circuit equation for i_{kd} with i_f treated as an input.

e result is

$$i_{kd} = -\frac{L_{md}\,p}{r_{kd} + L_{kd}\,p}\,i_f \tag{2.33}$$

s d-axis transient damper current will affect the torque since it will react with stator q-s current. Block diagram representation is given in Fig. 2.10 along with a sketch of the ponse to a step increase in i_f.

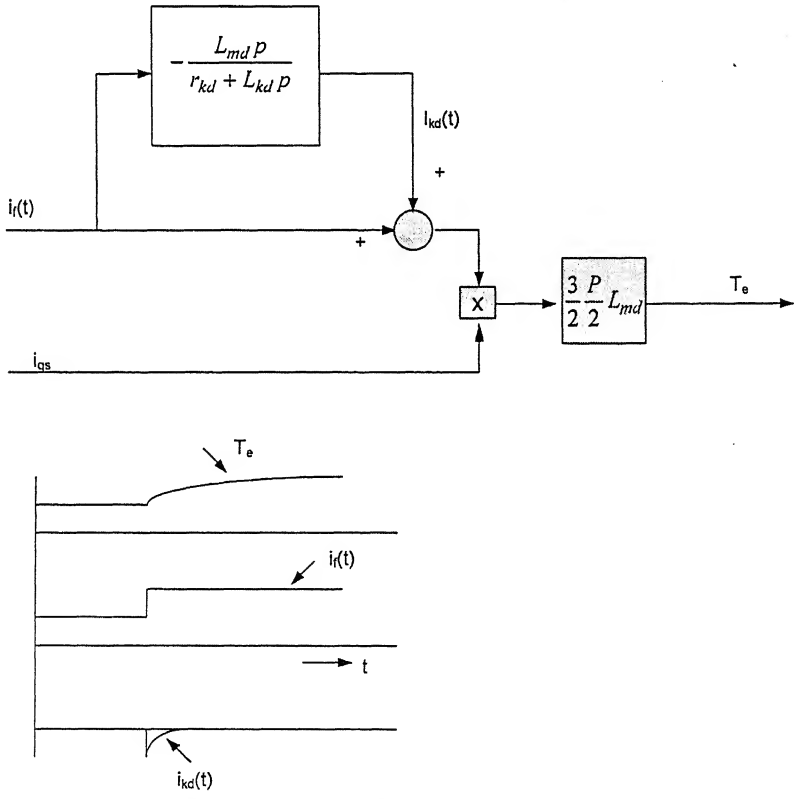

Fig. 2.10 Torque production for a change in field current in a field oriented synchronous machine ($\gamma=0$, $i_{ds}=0$)

This is identical to the situation in a dc machine since a step increase in dc machine field current will induce currents in the filed pole iron which must die away before the field flux can rise to its new value. This is precisely what happens in the field oriented synchronous machine except the induced current is treated as being in the damper circuit. Hence change in field current is associated with a delay in torque production.

2.5 Torque Control Implementations

The implementation of field orientation requires on-line computation of certain control variables using inputs from sensing elements, which continually sense operating motor variables such as motor line currents, motor shaft position and speed. These computed control variables serve as feedback values, which are compared with the appropriate reference values. The errors are continuously corrected by appropriately delaying or advancing the switching instants of the static inverter, from which the motor phases are fed. Thus implementation of vector control requires control of magnitude and phase of the stator current w.r.t location of the field winding axis. The vector control of the stator current must be maintained for both steady and transient conditions. Some of the possible implementation schemes are given below.

2.5.1. Torque Control using a CSI

Fig. 2.11(a) suggests a direct implementation of filed orientation ($\gamma=0$) using absolute position sensing and a CSI. With $\gamma=0$, the stator current is entirely q-axis current and is equivalent to a torque command. The rotor position information is directly utilized to set $\gamma=0$ by controlling the inverter firing times. Because of commutation delay inherent in CSI, some form of compensation is necessary to maintain $\gamma=0$ for different levels of current and different operating frequencies. This compensation is suggested in Fig.

.11(a) by the commutation delay compensation block and by inclusion of a phase egulator block. To operate at other than γ=0, a γ* command could be entered in the hase regulator. In this case the input current would no longer represent a torque ommand since it would contain both a q-axis and a d-axis component.

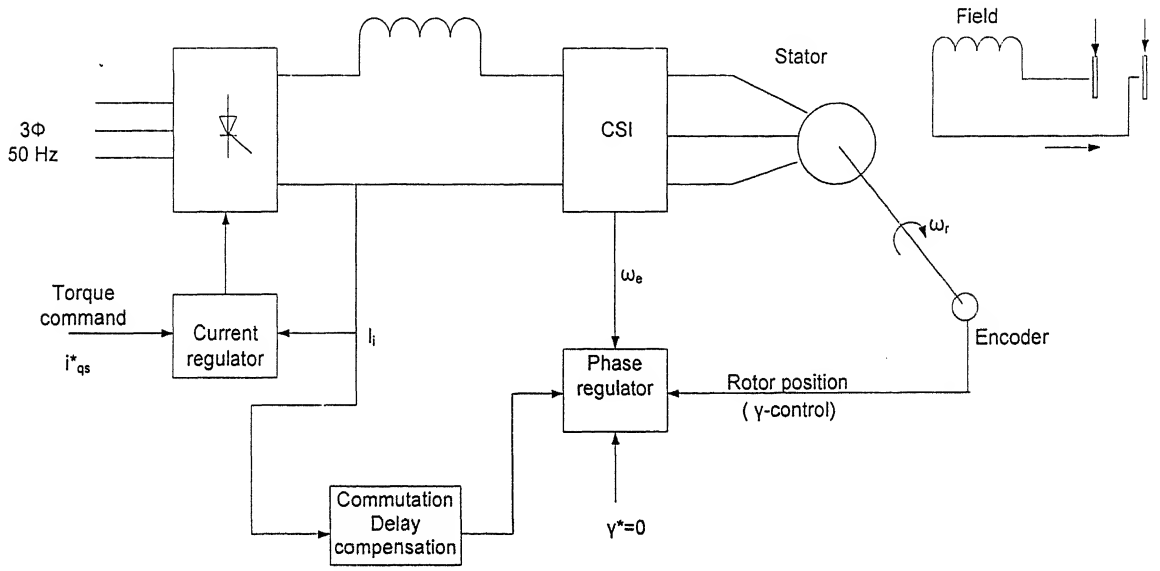

Fig. 2.11(a) Torque control via field orientation using a current regulated CSI.

2.5.2. Torque control using a CRPWM Inverter

The regulation of stator current by means of a fast switching power converter provides a simple means for implementing torque control with independent q-axis and d-axis current inputs. Fig. 2.11(b) illustrates a current regulated pulse width modulated inverter. In essence, all that required is to use absolute rotor position information to convert i^*_{qs} and i^*_{ds} commands in the rotor reference frame to a stator reference. The stator referred currents, at stator frequency, become the current commands for the CRPWM as shown in

Fig. 2.11(b). Normal field orientation is obtained by simply setting i_{ds}^{*}=0.Other choices for i_{ds}^{*} allow for controlling the motor power factor or other performance features. The rotor to stator transformation converts the dc signals representing the torque command i_{qs}^{*} and the field component command i_{ds}^{*} which become the current commands for the CRPWM .The actual equations implemented in the rotor to stator transformation block in Fig. 2.11(b) are the equivalent of the combined *rotating to stationary transformation and the two phase to three phase transformation*

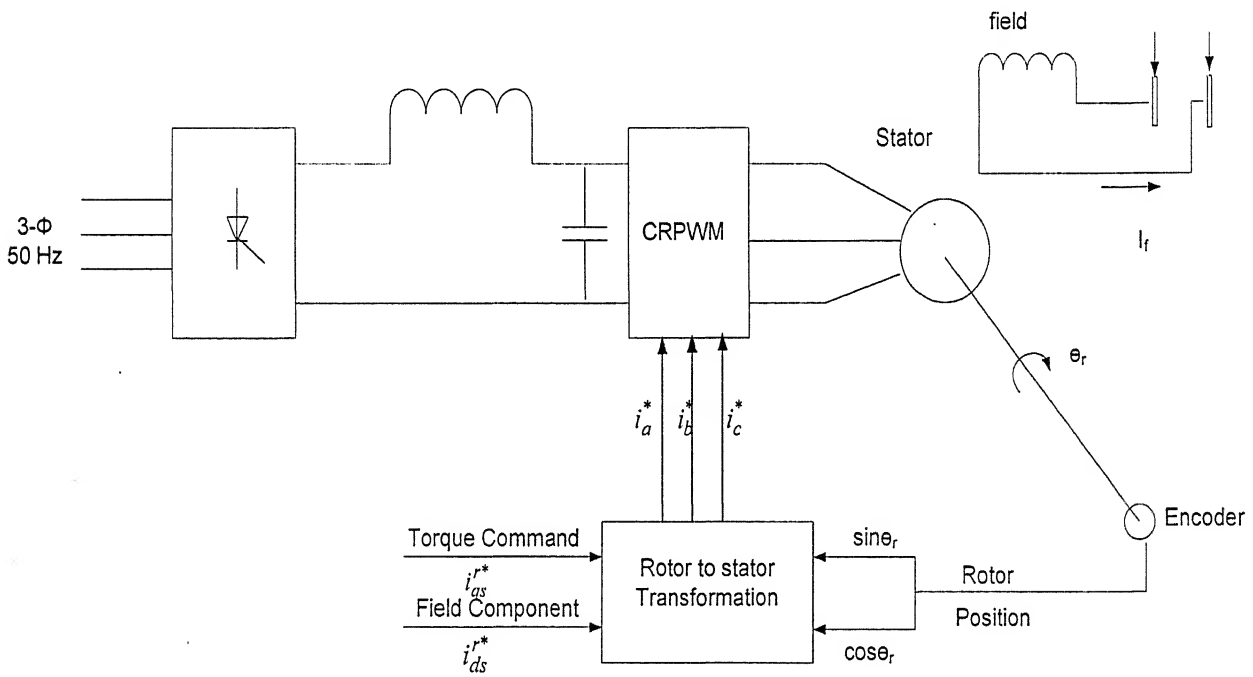

Fig. 2.11(b)Torque control using a CRPWM

2.5.3 Torque Control Requirements

The vector controlled synchronous machine systems of above figures can be interpreted in terms of basic torque control requirements of dc motor.

For the field oriented case of $\gamma = 0$ examination of figures reveal that

1. Current amplitude regulator provides an independently controlled armature current
2. The field winding is the exact counterpart of dc machine field winding.
3. The rotor position feedback loop controlling the phase of the stator current provides the field orientation such that the field flux and armature MMF are maintained in a mutually perpendicular orientation independent of rotor speed.

The only difference between the CSI fed system and the CRPWM system is that the separate amplitude and phase controls of the CSI are combined into a single instantaneous current controller in the CRPWM inverter and both functions are handled simultaneously. Thus the CRPWM inverter handles both the amplitude and angle of stator current necessary for torque control in a single operation.

2.6 Current Regulated PWM inverter

A current controlled PWM inverter operated with a switching frequency in the kHz range can function as a regulated current supply with the potential for good dynamic response and low harmonic content. It is the most commonly used in low to medium power range of high performance drives. Unlike the CSI, the PWM is a natural voltage source and conversion to current source operation requires closed loop control with feedback directly from the controlled ac currents. The feedback current sensors must therefore have a wide bandwidth, from the lowest fundamental frequency to be controlled to somewhat above the PWM carrier frequency. Fig. 2.12 illustrates the basic system.

This system has several fundamental differences from the CSI system including:

1. The requirement of an actual time domain reference instead of the amplitude and phase references required in the CSI.

2. The possibility of reducing harmonic content to arbitrarily small values as the PWM frequency increases.
3. The need for a current regulator operating with ac signals as opposed to the dc regulator of the CSI.
4. The need for wide bandwidth current sensors.

The excellent response and low harmonic content of the PWM system makes it the best currently available regulated current supply. Basically the regulator must function to convert the time domain current error signals to firing signals for the PWM inverter .The dual function of error processing and subsequent conversion to gate drive signals is required in all types of regulators. Current regulators are generally classified into three categories: 1.Hysteresis regulators, 2. Ramp comparators, and 3. Predictive controllers.

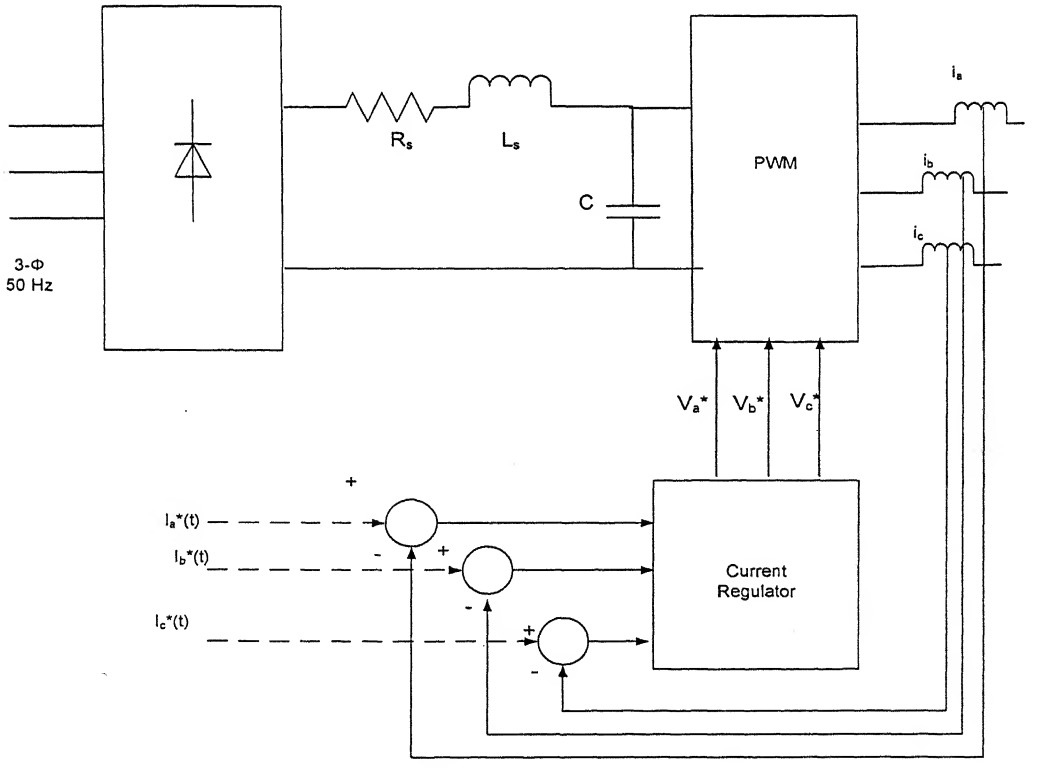

Fig. 2.12 PWM system with current regulation to produce a controlled three phase current source

2.7 Hysteresis Regulators

The basic concept of this type of controller is illustrated in Fig. 2.13 (a).

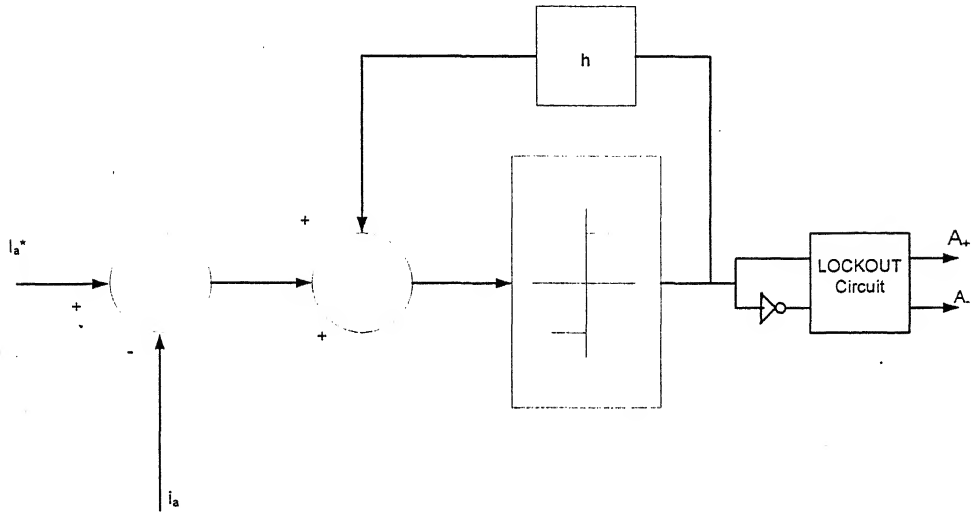

Fig. 2.13 (a) Hysteresis current controller for one phase

The controller simply applies the current error signal to a hysteresis element, the output of which supplies the logic signal to gate the positive or negative inverter switching element lockout circuit is normally incorporated to allow for inverter switch recovery time and thus avoid short circuits across dc link

While this system is very simple and provides good current amplitude control, hysteresis regulation has the major disadvantage of producing a highly variable PWM switching rate. Low frequencies appear in the spectrum regardless of the switching frequency .The variation of switching rate is also opposite to the needs for good current control with highest switching rates associated with lowest reference frequencies. The hysteresis controller also has somewhat unexpected property of limiting the current error to twice the hysteresis band (2h) rather than to the band (h) itself.

If i_a is actual current and i_a^* is reference then referring to Fig. 2.13 (b) it can be written as

$$i_a > i_a^* + h \quad \text{then} \quad Vao = 0$$

$$i_a < i_a^* - h \quad \text{then} \quad Vao = V_{dc} \qquad \text{and}$$

$$i_a^* - h < i_a < i_a^* + h \quad \text{then Vao maintains its previous state.}$$

Similarly it can be written for other two phases also. These conditions form the basis for modeling of 3-phase hysteresis controller.

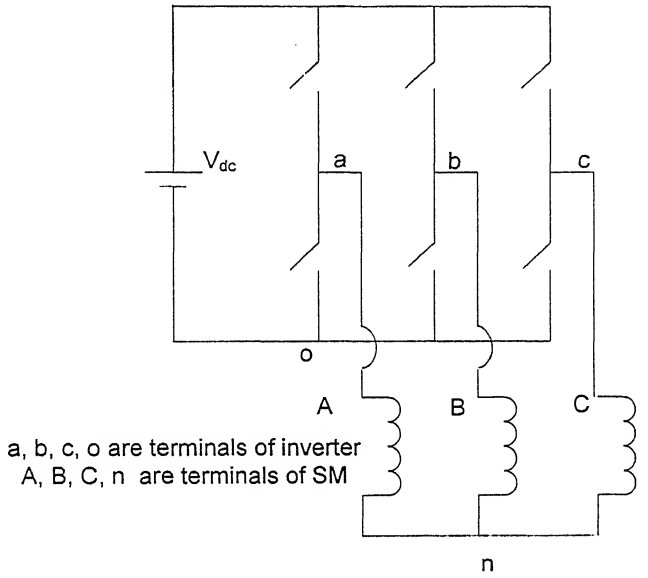

Fig. 2.13 (b) Inverter – SM system

Then phase voltages of SM can be written as

$$V_{AN} = V_{ao} - V_{no}$$

$$= \frac{1}{3}[2V_{ao} - V_{bo} - V_{co}] \qquad 2.34$$

similarly

$$V_{BN} = \frac{1}{3}[2V_{bo} - V_{co} - V_{ao}] \qquad 2.35$$

$$V_{CN} = \frac{1}{3}[2V_{co} - V_{ao} - V_{bo}] \qquad 2.36$$

Inverter was modeled on the basis of the equations 2.34, 2.35 & 2.36.

2.8 Digital Simulation:

This section deals with digital simulation of CRPWM–SM drive for various conditions of speed and torque. The Vector controller SM drive was modeled using equations discussed in previous sections. The simulation of system is carried out using **Matlab 6.5 Simulink.** Vector controlled SM drive system is simulated for speed reversals and torque changes.

Response of a normal synchronous motor starting from rest against a constant load torque of 4 N-m for a speed command of 157.1 electrical rad/s is as shown in Fig. 2.14.

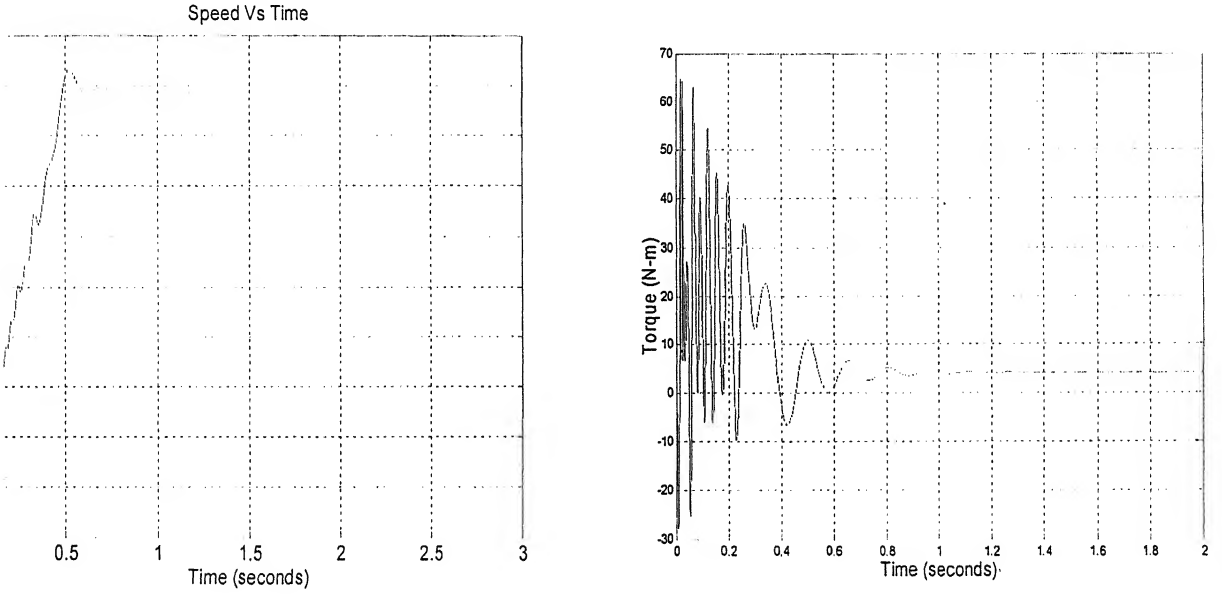

Fig. 2.14 Simulation response of a normal SM starting from rest against a constant load torque

2.8.1 Step change in speed and torque: At t =0, a speed command of 157.1 *electrical rad/s* (750 rpm) against a load torque of 4 *N-m* is applied. Fig. 2.15 shows the response for a normal SM and a Vector controlled SM drive.

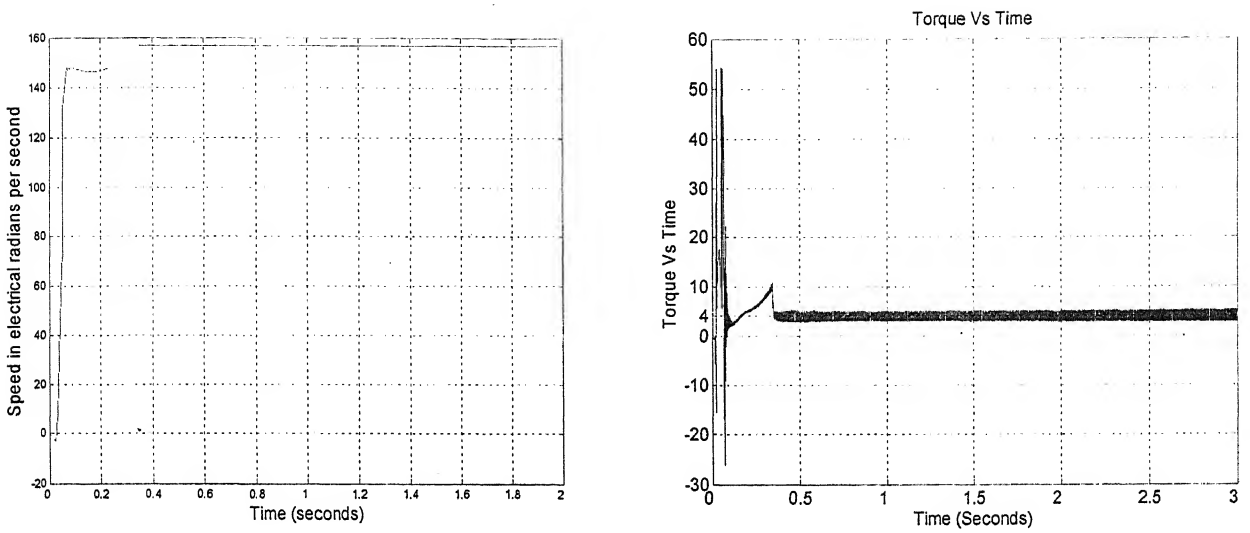

Fig. 2.15 Response of Vector Controlled SM for a step change in speed and torque.

2.8.2 Speed Reversal: A step speed reversal from +157.1 to -157.1 elec. rad. /s at t = 1s.

The response of vector controlled SM for speed reversal is as shown in Fig. 2.16.

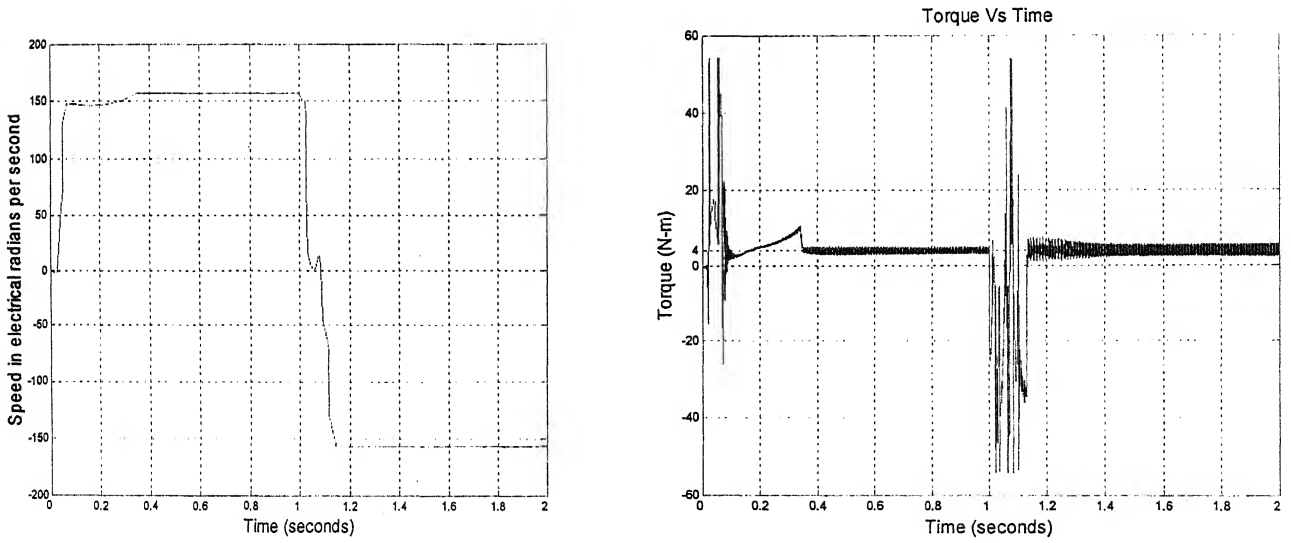

Fig. 2.16 Response of Vector Controlled SM for speed reversal.

2.8.3 Change in torque: The motor is subjected to a reversal of load torque while its speed is kept constant. At t = 2s, load torque is reversed from + 4 N-m to -4 N-m. Vector controlled drive took less than 0.1 s as shown in Fig. 2.17.

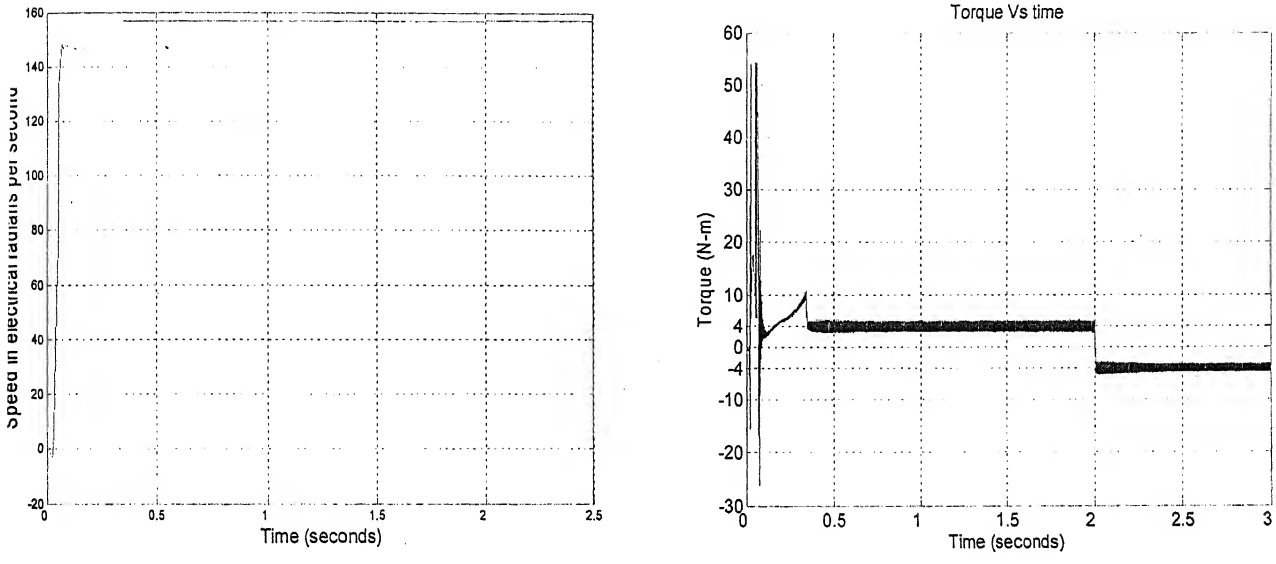

Fig. 2.17 Response of a Vector Controlled SM drive for change in torque.

2.8.4 Four Quadrant Operation: The motor is subjected to both speed and torque reversals. At t = 1s speed is reversed from + 157.1 to -157.1 elec.rad/s. Further at t = 2 s torque is reversed from + 4 N-m to -4 N-m. The response of a vector controlled SM drive is as shown in Fig. 2.18. Phase currents of A, B and C are as in Fig. 2.19. The phase voltages of inverter are as shown in Fig. 2.20. It can be concluded from Fig. 2.21 that drive system is operating in lagging power factor. Reference and actual current waveforms are as shown in Fig. 2.22 (a) & (b) with operating value of h = 0.2 A.

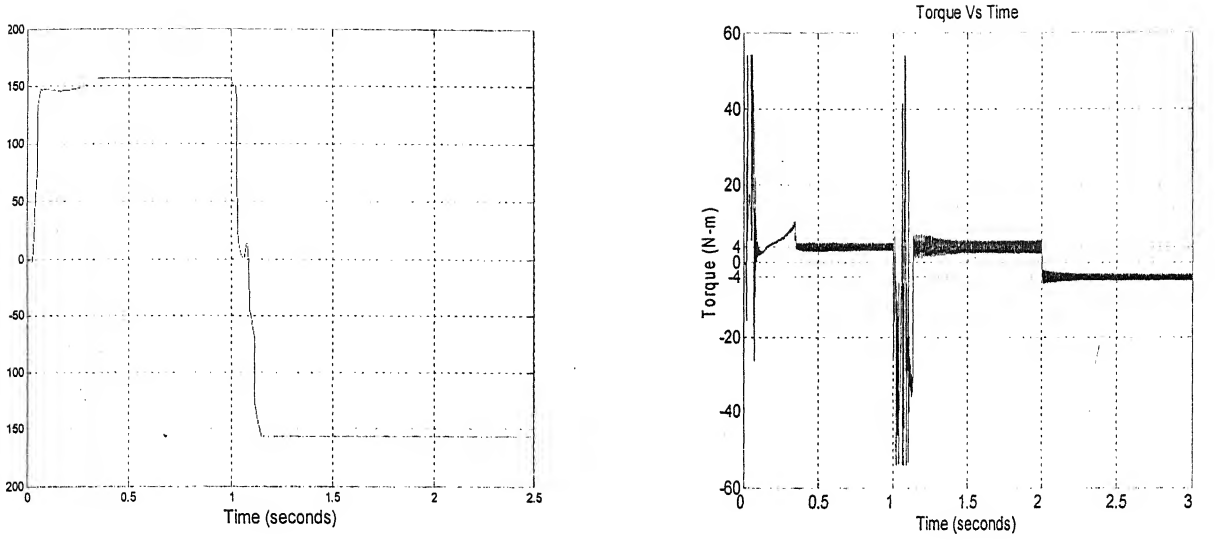

Fig. 2.18 Response of Vector Controlled SM drive for speed and torque reversals.

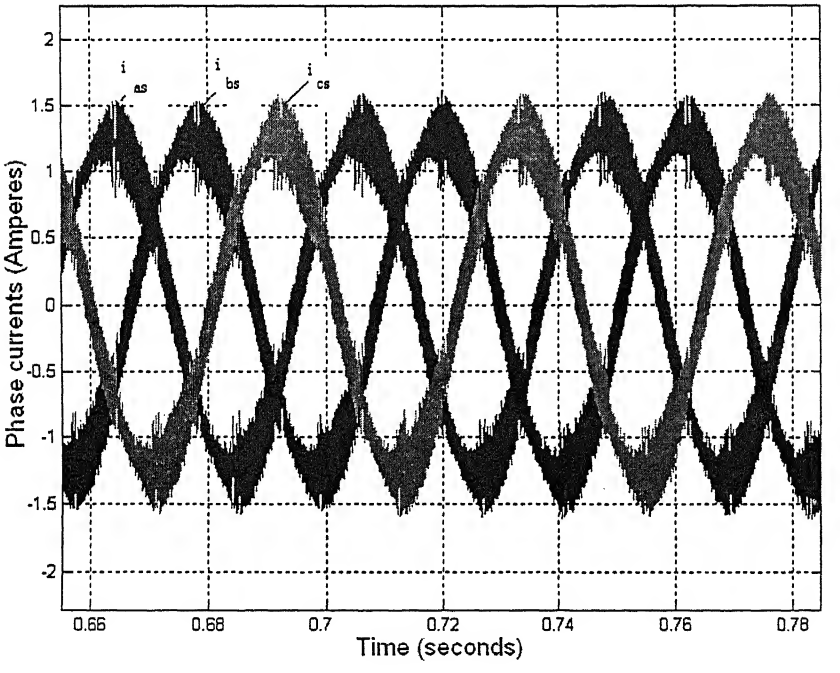

Fig. 2.19 Phase currents of Vector controlled SM drive.

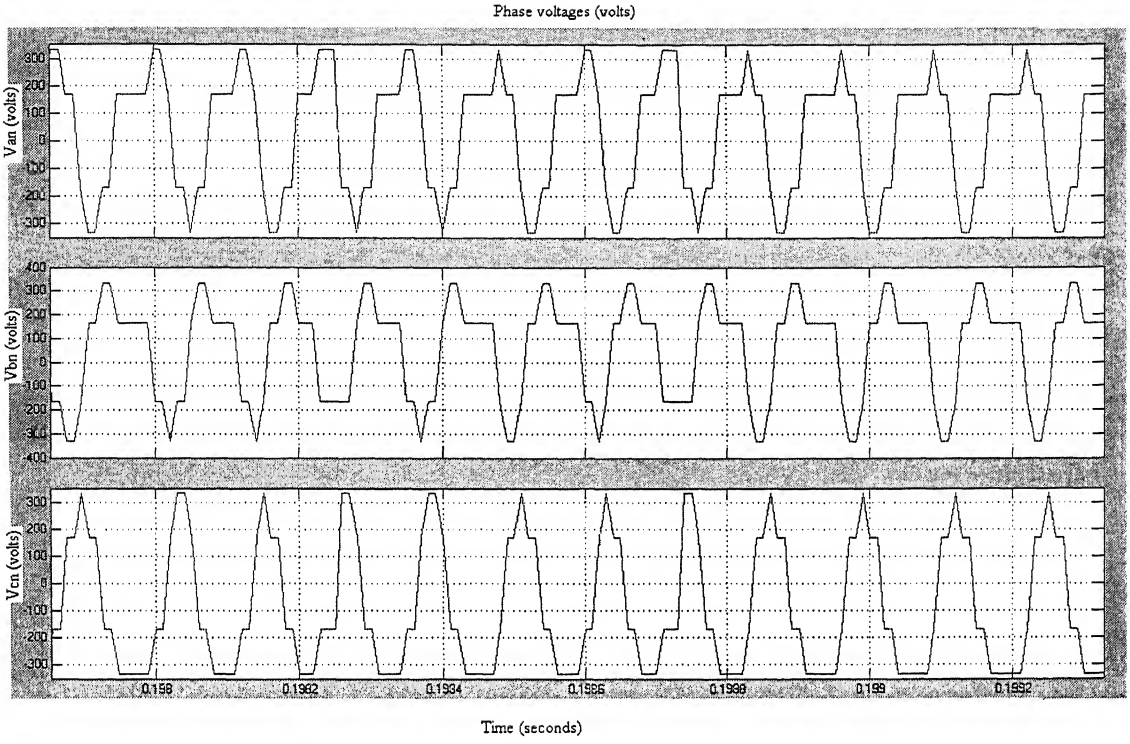

Fig. 2.20 Phase voltages of Inverter.

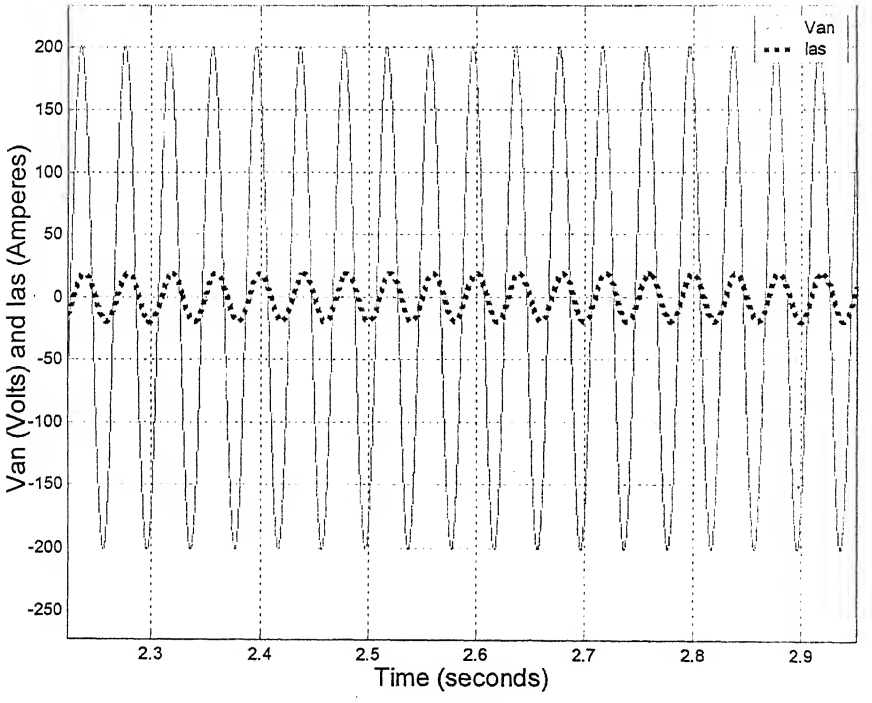

Fig. 2.21 Waveform showing Van and Ias (Ias scale is multiplied by 10 times).

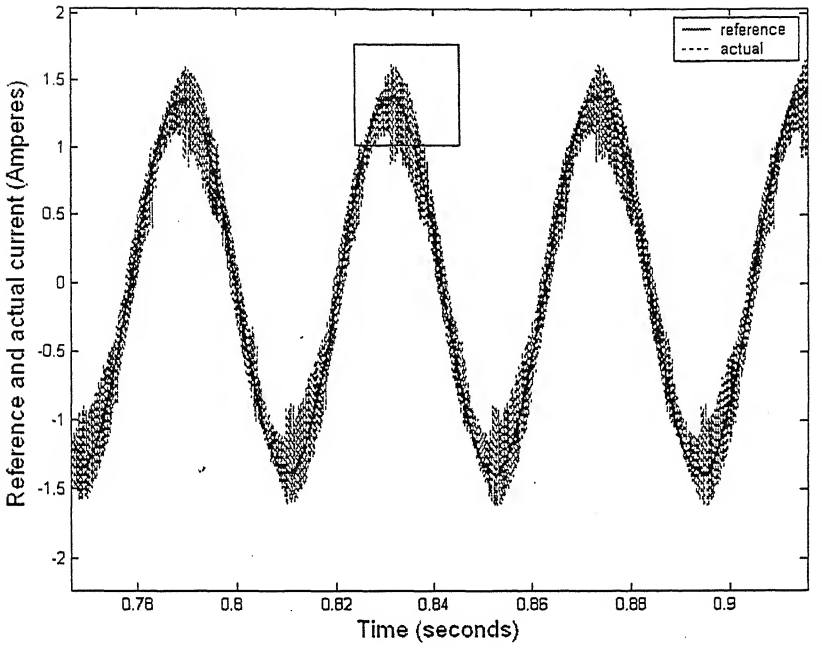

Fig. 2.22(a) Waveform showing Reference and actual currents of phase-A

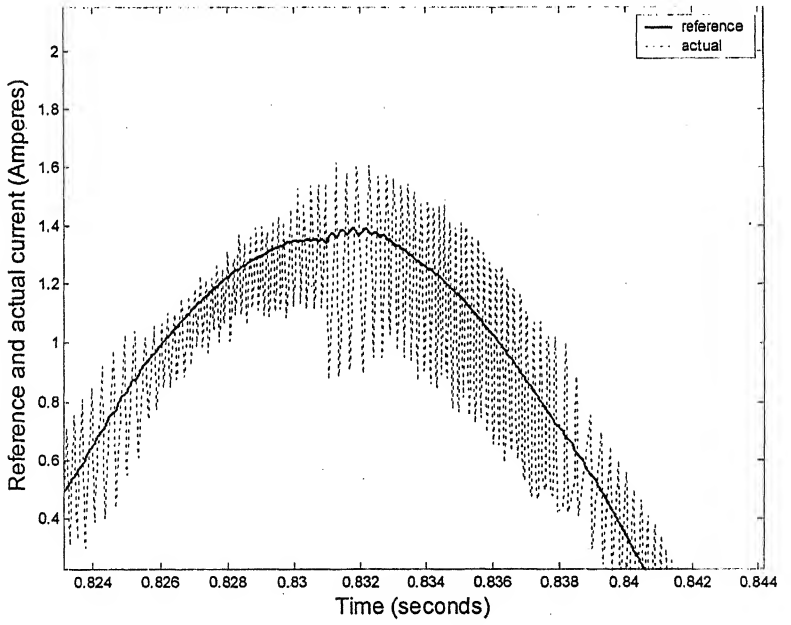

Fig. 2.22 (b) Reference and actual currents (zoomed-one of above figure)

2.9 **Conclusions**

Modeling of Vector controlled SM (with $i_{ds} = 0$) drive using d-q axis theory is done. Simulation of drive for change in speed and torque, speed and torque reversals has been made. Corresponding plots of various parameters are plotted. The speed and torque response of a vector controlled SM drive are found to be good.

Chapter -3

PC-Based Implementation of the Vector Controlled SM Drive

3.1 Introduction

This chapter gives the detailed description about the fabrication of circuit and experimental setup done in the laboratory. It initially focuses on the different aspects of experimental setup and then looks at the different test conditions employed on the drive system. Corresponding results for different test conditions were also presented.

Drive was run on basis of field orientation principle in which the spatial angle between rotor flux and torque producing component (i_{qs}) of stator current is controlled and held at 90°. With $i_{ds} = 0$, the required 90° spatial angle between the field flux and the stator mmf for field orientation is maintained as explained in section 2.4. This (instantaneous d-axis stator current is zero) inherently requires field (flux) position information since the current must be controlled w.r.t the rotating rotor reference frame. Field position information is known all times by using rotor position feedback. The drive is run with field voltage kept constant. As explained in section 2.4, with field voltage kept constant there is a complete decoupling of d-axis from stator windings and response of drive is as good as a separately excited dc motor.

The block diagram of experimental setup is as shown in Fig. 3.1. Inverter is fed from a three phase rectified supply and operated in a current controlled mode. Hysteresis controller is used to operate it as a CRPWM inverter.

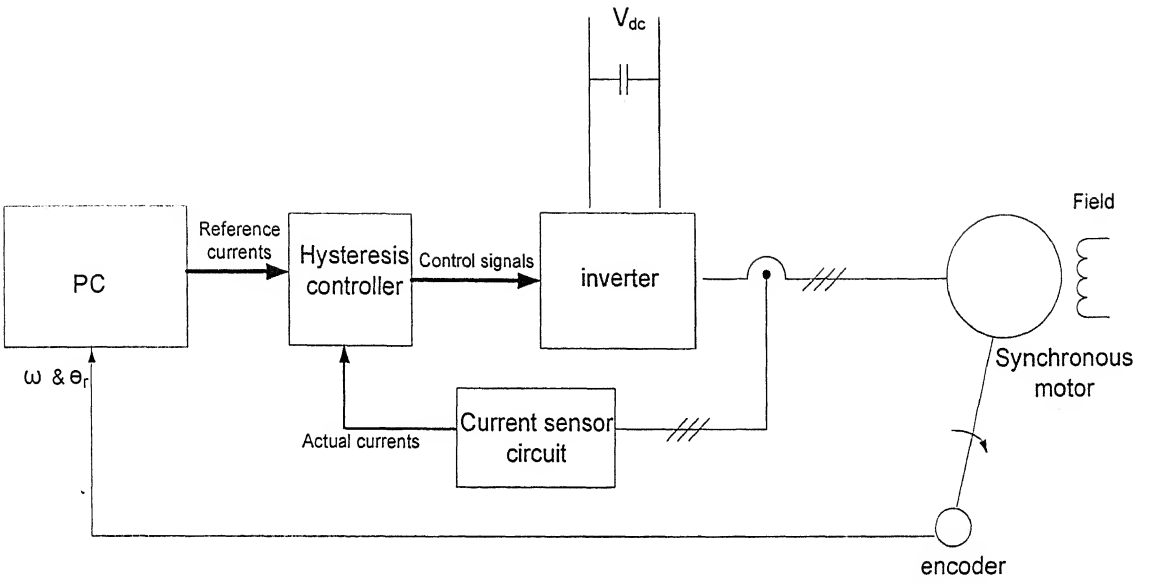

Fig. 3.1 Block Diagram of laboratory setup.

Speed, direction and rotor position angle (θ_r) measured from encoder are given to the computer. An algorithm developed on field orientation principle uses these inputs and generate reference currents. The hysteresis controller compares reference current and actual current, its output is used to drive the inverter.

3.2 Inverter Power and Control Circuit Fabrication

The power circuit consists of a 3-phase inverter built using Mitsubishi IGBT modules. Each module has a pair of IGBT's rated for 50 A (I_C) and 1200 V (V_{CES}). Mitsubishi hybrid IC [17] is used for driving gate of IGBT. The hybrid driver IC provides the required isolation between input and output using an opto-coupler. It also provides short circuit protection by a built in desaturation detector. A fault signal is provided if the short circuit protection is activated. Driver circuit diagram for phase A is as shown in Fig. 3.2.

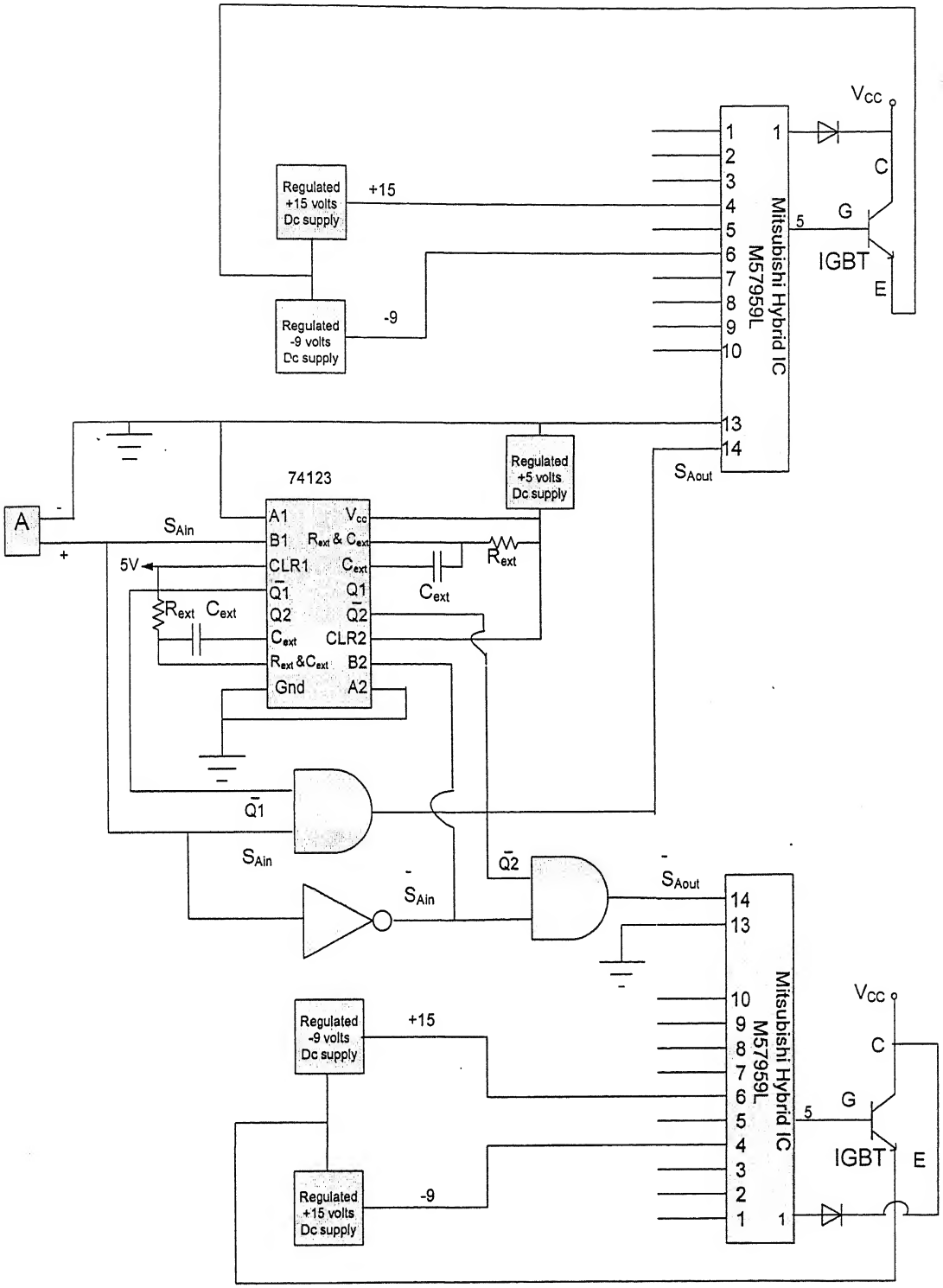

Fig. 3.2 Driver circuit diagram for phase-A.

The IGBT drive circuit consists of a lockout circuit, hybrid ICs and their power supplies. Lock-out circuit provides delay to S_{Ain} and $\overline{S}_{Ain}$ to avoid the shoot-through fault due to simultaneous turn-on of both the upper and lower switches in same leg. Selection of proper values of R_{ext} (665Ω) and C_{ext}(0.01μf) in retriggerable monostable chip 74123 controls the delay. With these chosen values, the observed delay is 5μs.The actual signals that are amplified by the hybrid ICs, are S_{Aout} and $\overline{S}_{Aout}$.Driver circuit also has regulated isolated dc power supplies of +15V, -9V for driver cards and a +5V for IC's. Hysteresis controller provides the signal S_{Ain} to inverter.

All the IGBT's along with their driver circuits and transformers are enclosed in a box. The 3-phase output terminals and input dc terminals are taken out of the box. A few snaps of the inverter built in the lab are presented here.

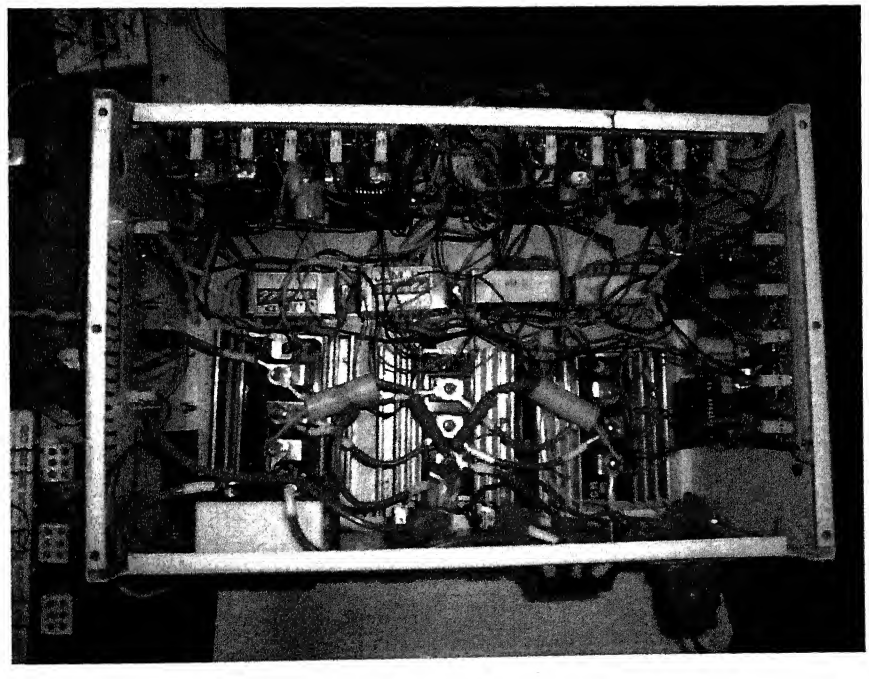

Fig 3.3 Inner View of Inverter (from top).

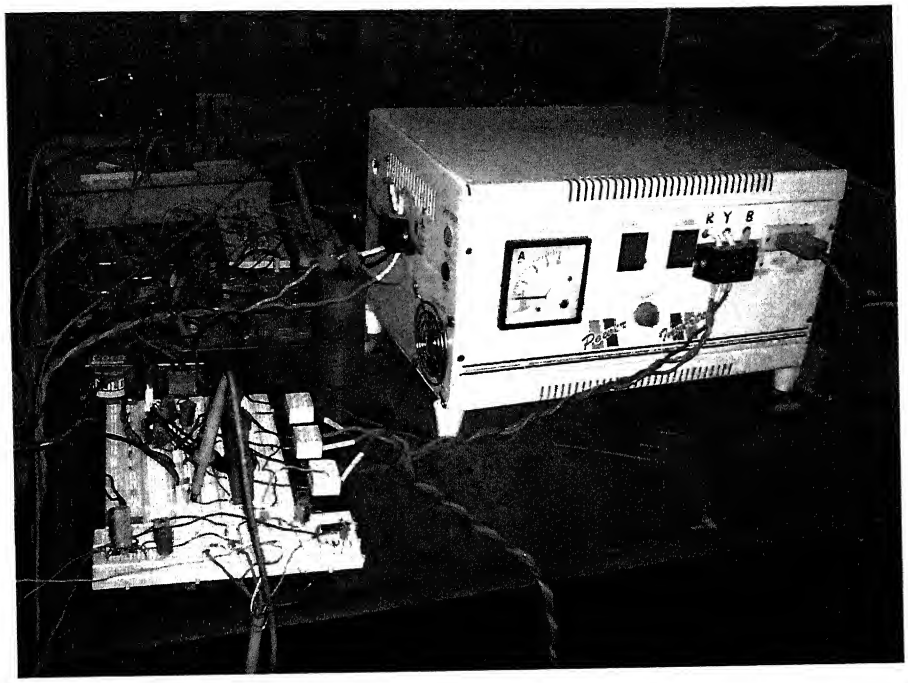

Fig 3.4 View of Experimental setup. (Inverter and control circuit).

Fig 3.5 Another view of experimental Setup.

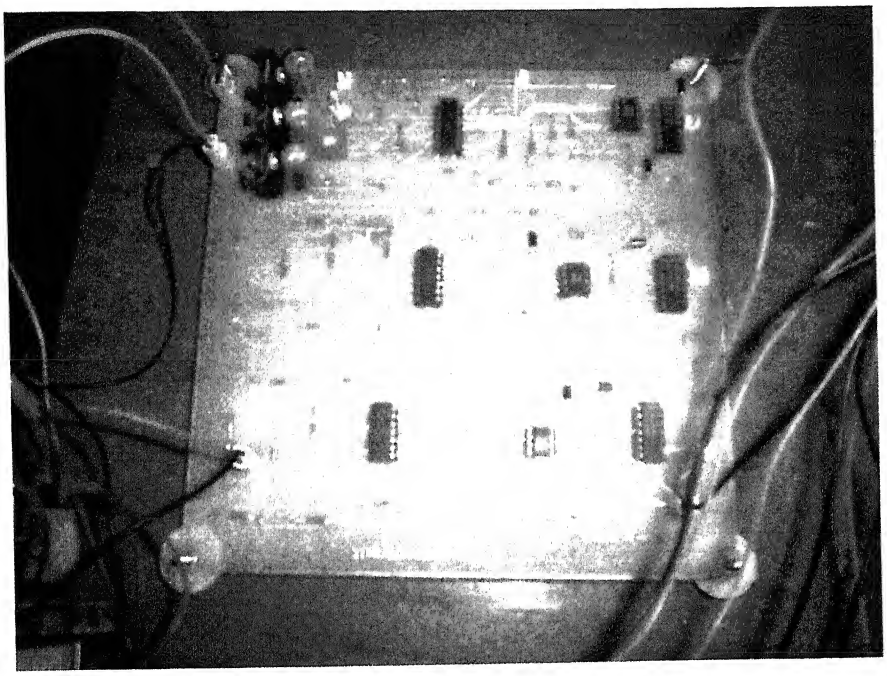

Fig 3.6 Hysteresis Controller Circuit.

Fig 3.7 Synchronous motor and dc generator load.

3.3 Hysteresis Controller

The hysteresis circuit is designed using TL084 (quad op-amp). A potentiometer is used to adjust the hysteresis band (h). The hysteresis current controller, which keeps the armature current within a band, is as shown in Fig. 3.8. Op-Amps C1, C2 and C3 establish the hysteresis window ($i_s^* \pm h$) around the reference current i_s^*.The window height (h) is controlled by the potentiometer P1 (5 kΩ). C4 and C5 compare the armature current i_s with the lower and the upper bands respectively [18]. The output of C4 is connected to the S terminal of S-R flip-flop. The output of flip-flop Q acts as S_{Ain} signal, which is used to trigger the positive group of IGBT.

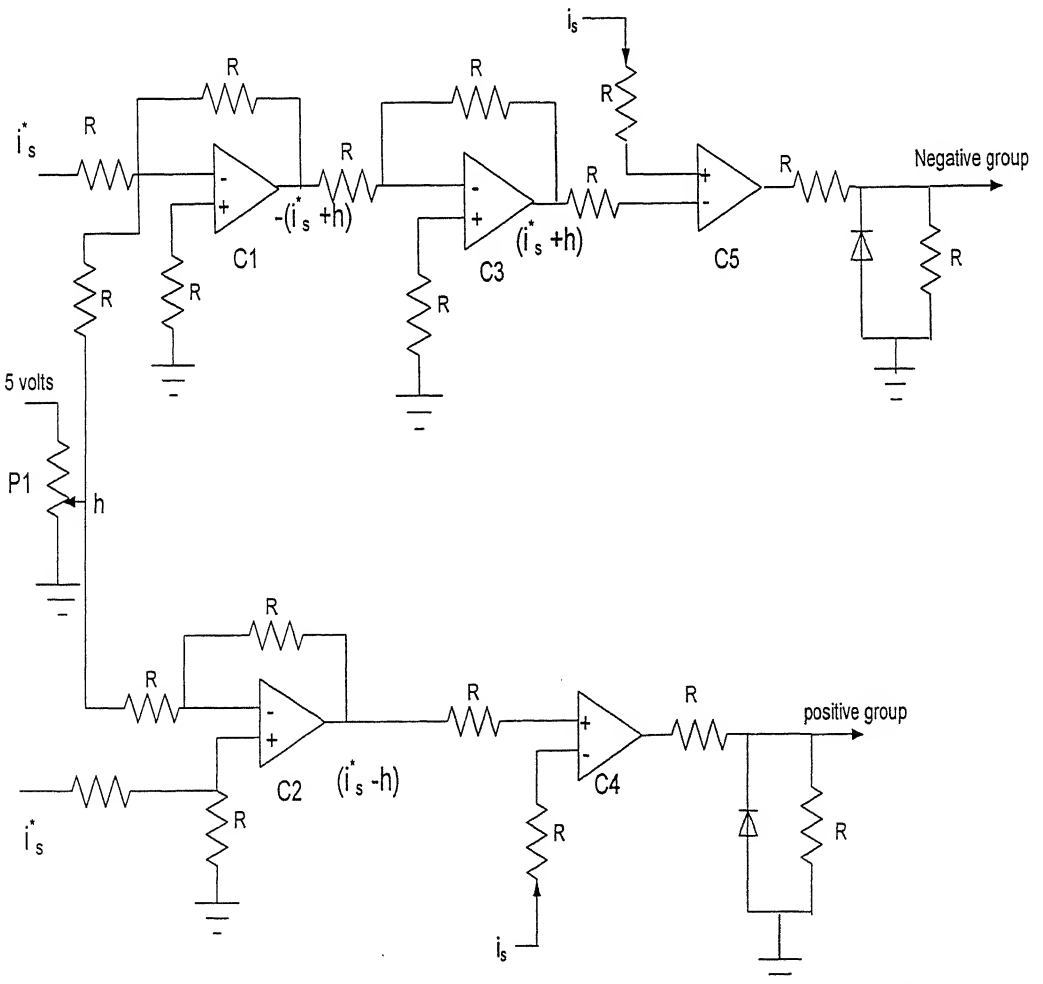

Fig. 3.8 Hysteresis Current Controller Circuit Diagram. (R =2.2 kΩ)

3.4 Current Sensors

The armature current signals of SM are required for implementation of hysteresis controller. LEM's LA 55-P was used for sensing the phase currents of SM. The circuit diagram is as shown in Fig. 3.9. The current sensor was wound with 7 turns for a full load current of 7 amperes. The voltage across R_M is the measure of current in the circuit. R_F and C_F act as the filter. The scaling factor of the current sensor with R_M (100Ω) is found to be 1 A = 0.692 Volts.

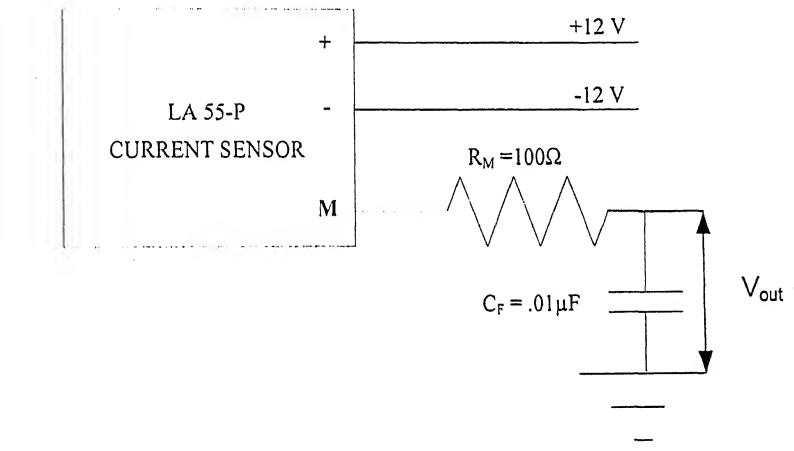

Fig. 3.9 Current Sensor Circuit.

3.5 Encoder

In a self controlled synchronous motor drive system, precise rotor position is required to control the power converter in synchronism with rotor. Speed signal is usually obtained digitally by counting the pulses coming out of an encoder mounted on the shaft. Among the position / speed sensors available, absolute *and incremental* encoders are commonly used in practice. Absolute encoders give direct information for each rotor position and the position information does not get lost with power failure. But the absolute encoders are costly, cannot be made compact due to increased number of

output signal wires, and the least count is limited by the number of output bits. On the contrary, the incremental encoders are comparatively more rugged, and now high resolution incremental encoders are available at reasonable prices. The problem faced while using incremental encoders is that they generate only a pulse train with a frequency dependent on speed of rotation for either directions of rotation, from which the position information needs to be extracted. In the present work, a high resolution incremental encoder, as available, is used with 2500 pulses/revolution. The encoder generates two pulses in quadrature (2500 pulses /revolution) and a marker pulse (1 pulse / rev.) along with their complements which are symbolically denoted by (K_1, K_2, K_0, $\overline{K}_1, \overline{K}_2, \overline{K}_0$) respectively as shown in Fig. 3.10 (a). With help of PC interface and a C program, accurate position information is found out for all possible conditions including repetitive speed reversals within a revolution, thus emulating the performance of an absolute encoder.

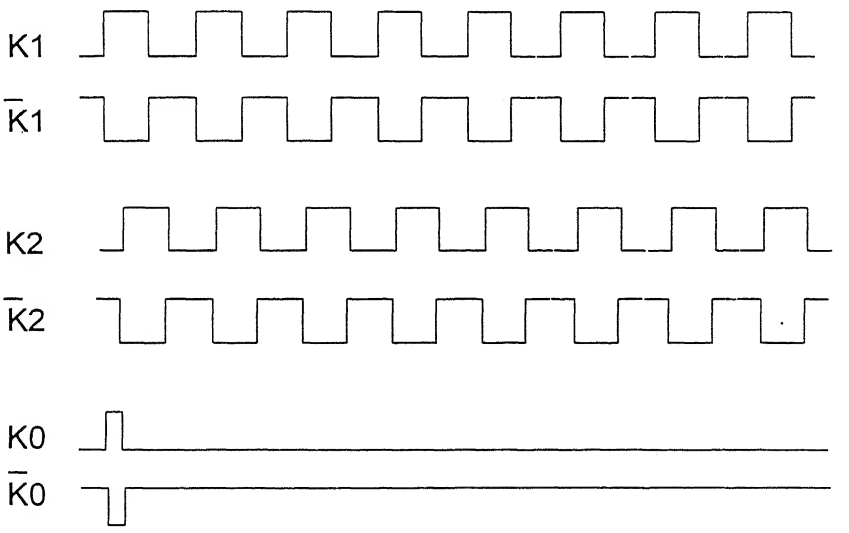

Fig. 3.10 (a) Typical output signals of the encoder at constant speed.

3.6 PC Interface

The drive is controlled using an Intel Pentium-III, 600 MHz, 128 MB RAM computer. Analog and digital signal interfaces are achieved by means of two add-on cards mounted on PC expansion slot. They are ACL-8112 PG (Enhanced Multi-function Data Acquisition Card) and PCL-223 (Multi-function Timer/Event Counter Card with DI/O and VFC) manufactured by AD Link and Dynalog Micro systems respectively. The detailed specifications of both the cards are given in the Appendix. No commercially available driver for the cards is used as both of them are generalized and written in high level languages such as BASIC and C. An algorithm based on vector control principle (constant field control) was developed and program was written in C-language for the same. The program is given in Appendix.

3.6.1. Speed Measurement

The speed is measured is made by the well known m/T method [19]. The formula for speed is given by

$$\text{Speed in Electrical radians/s} = \frac{C}{2500} * \frac{P}{2} * \frac{2\pi}{T_s} \qquad (3.1)$$

where C = no. of pulses in one sampling period.

P = no. of pulses.

T_s = sampling period.

Counters of PCL -223 card are used to find out the values of C and T_s. 8254(A0) and 8254 (C0) in are used in calculation of T_s and m respectively. Both counters are programmed in mode-0 (event counting) and their gate is enabled by software. The clock to counter A0 of 8254 is fed with a pulse train of 1MHz from a crystal oscillator housed in PCL-223. The encoder pulse train K_1 acts as clock to counter C0 of 8254.

Both counters are loaded with OXFFFF at the beginning of loop, which decrement with the pulses coming to their clocks. At the end of loop the counters are latched, the count value is read and the number of pulses is evaluated. The speed is calculated using the equation (3.1).

3.6.2. Direction Measurement

The direction of rotation of the motor is found out using the pulses K_1 and K_2 which are in quadrature with each other. K_1 is fed to the clock and K_2 to the D input of D flip-flop. Output Q goes high for forward direction and goes low for reverse direction of rotation that is sensed through the digital input port of CN1 of ACL-8112 PG (Fig. 3.10(b)).

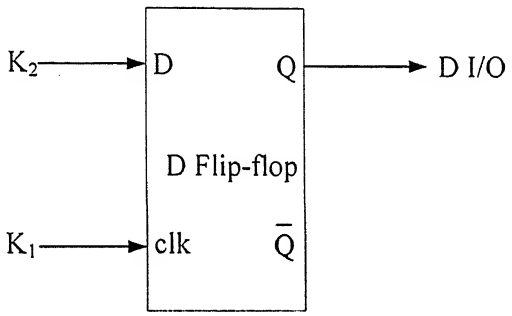

Fig 3.10 (b) Direction Measurement

3.6.3 Rotor position measurement

A mere counting of the incremental pulses does not necessarily give correct position information. Along with the pulse counting, the direction of rotation should be noted and the counting has to be reset periodically to avoid the loss of the position information either due to repetitive direction reversals or due to a cumulative error. For calculating rotor position K_1 is fed to clock of counter C1 of 8254 and K_0 as its gate. The pulse train K_1 has a frequency dependent on the speed but independent of the direction of rotation. K_0 gives a pulse once in a revolution and thus serve as the marker pulse,

which is to be aligned appropriately with the rotor position. So the pulses K_1 and K_0, pulses from encoder, and the direction information are used in association with software to emulate the performance of an absolute encoder with a good resolution. The encoder is so aligned that the arrival of the marker pulse corresponds to the physical alignment of the field with armature phase-A, and so, the marker reloads the counter C1 of 8254 with original count corresponding to $\theta = 0$. The counter is periodically reset by the encoder marker pulse eliminating the possibility of a cumulative position error.

Very often the shaft is subjected to mechanical oscillations which, if not accounted for, give rise to cumulative position error leading to the loss of angle information [20]. This situation can be generalized as multiple direction reversal within a mechanical revolution where the synchronizing marker pulse is not available for resetting the angle to a correct value. The program has been designed to tackle the above problem by keeping track of successive changes in the direction of rotation, thus giving the performance identical to that of an absolute encoder with good resolution.

3.6.4 Algorithm for rotor position measurement

1. signN =1, signO =1, dirP=0, dirN=0;
2. Find the counter value (Cn).
3. Bx = (0xffff-Cn)*4*pi/2500;
4. Check the direction of motor and assign its value to signN.

```
If (signN! = signO)
    CNT0 = Bx;
    TH0 = Theta;
```

dirN = 0;

dirP = 0;

5. If (signN = signO =1 and dirP = 0) // forward direction

Theta = Bx;

If Theta > 4*pi then Theta = Theta – 4*pi

6. If (signN= signO = 0 and dirN = 0) // reverse direction

Theta = 4*pi – Bx;

If Theta < 0 then Theta = Theta + 4*pi;

7. If (signN = 0 and signO = 1 or dirN =1) // forward to reverse

If (CNT0 > Bx) // if marker pulse has arrived

dirN = 0

else

Theta = TH0 + CNT0 –Bx;

If Theta < 0 then Theta = Theta +4* pi;

dirN = 1;

8. If (signN = 1 and signO = 0 or dirP =1) // reverse to forward

If (CNT0 > Bx) // if marker pulse has arrived

dirP = 0;

else

Theta = TH0 +Bx - CNT0;

dirP = 1;

9. signO = signN;

where

signN, signO are the directions in present and previous iterations.

dirP = 1 at the time direction changes from reverse to forward and gets reset to 0 after either marker pulse is encountered or dirN=1;

dirN= 1 at the time direction changes from forward to reverse and gets reset to 0 after either marker pulse is encountered or dirP =1;

Cn is content of counter irrespective of direction...

Bx is position of rotor in electrical radians.

CNT0 is assigned to Bx at the time of reversal.

Theta is actual value of rotor position taking direction into consideration in electrical radians.

TH0 is assigned to Theta at the time of reversal.

3.7 Algorithm for Vector Control of SM (with $I_{ds} = 0$)

The following algorithm is used for vector control of SM (with constant field control)

1. Measure the rotor angle (theta).
2. Measure the rotor speed.
3. Calculate the speed error.
4. Calculate the PI controller output using speed error.
5. The output of PI controller forms the I_{qs} component
6. $I_{as} = -I_{qs} * \sin(\text{theta})$;

   $I_{bs} = -I_{qs} * \sin(\text{theta} - 2\pi/3)$;
7. Output I_{as}, I_{bs} then through D/A converters.

3.8 Test Results

The experimental CRPWM Inverter–fed vector controlled SM drive is subjected to different test conditions. The 3-phase auto transformers prior to the rectifier bridges feeding inverter and field winding are adjusted to obtain suitable line voltage depending upon the operating speed. For present experiment, the dc link voltage of inverter is adjusted to 25 V and the field current is adjusted to 0.3 A and kept constant. Band of hysteresis controller was kept at 0.3 V.

Controller circuit consisting of IGBT drivers, hysteresis controller are energized. The rotor position was adjusted such that it is at zero degree position. (The zero degree position of rotor was set such that arrival of marker pulse corresponds to the physical alignment of the field with armature phase-A.) After adjusting rotor to zero degree position, the main C-program was run on PC in DOS mode. Then mains switch of inverter is switched on. This initiates the starting process. The typical results of experimental set up are recorded using a storage oscilloscope (Tektronix, TDS 1012, and 100 MHz).

A speed command of 150 r/min is given. Fig. 3.11 shows the experimental result showing the response of motor speed. Fig. 3.12 (a) shows the reference current and actual current of phase-A while Fig. 3.12 (b) shows the line-line voltage V_{AB} in transient period. At t = 0, the speed command was given. It can be seen from Fig. 3.12 that steady state was attained by 0.75 seconds. The steady state values of current and voltage are shown in Fig. 3.13 (a) & (b) respectively. The load current is 2 amperes per phase and line-line r.m.s voltage is 22 V.

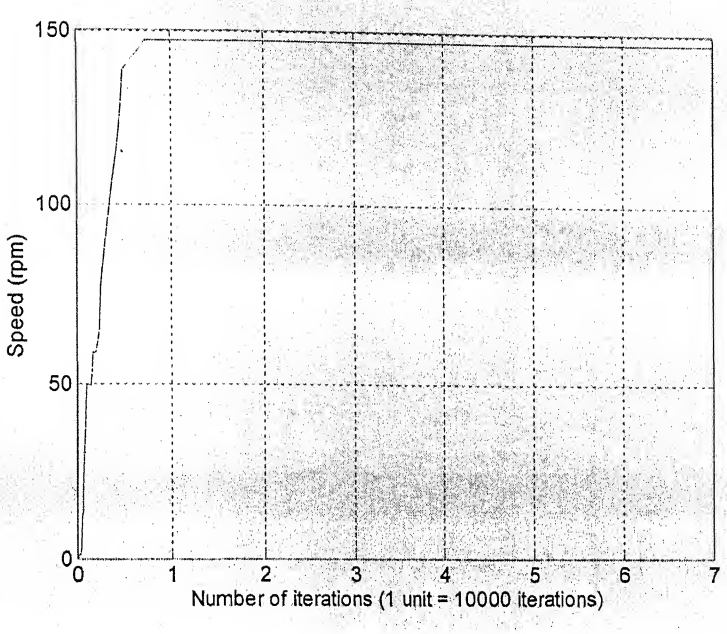

Fig. 3.11 Speed response for speed command of 150 rpm.

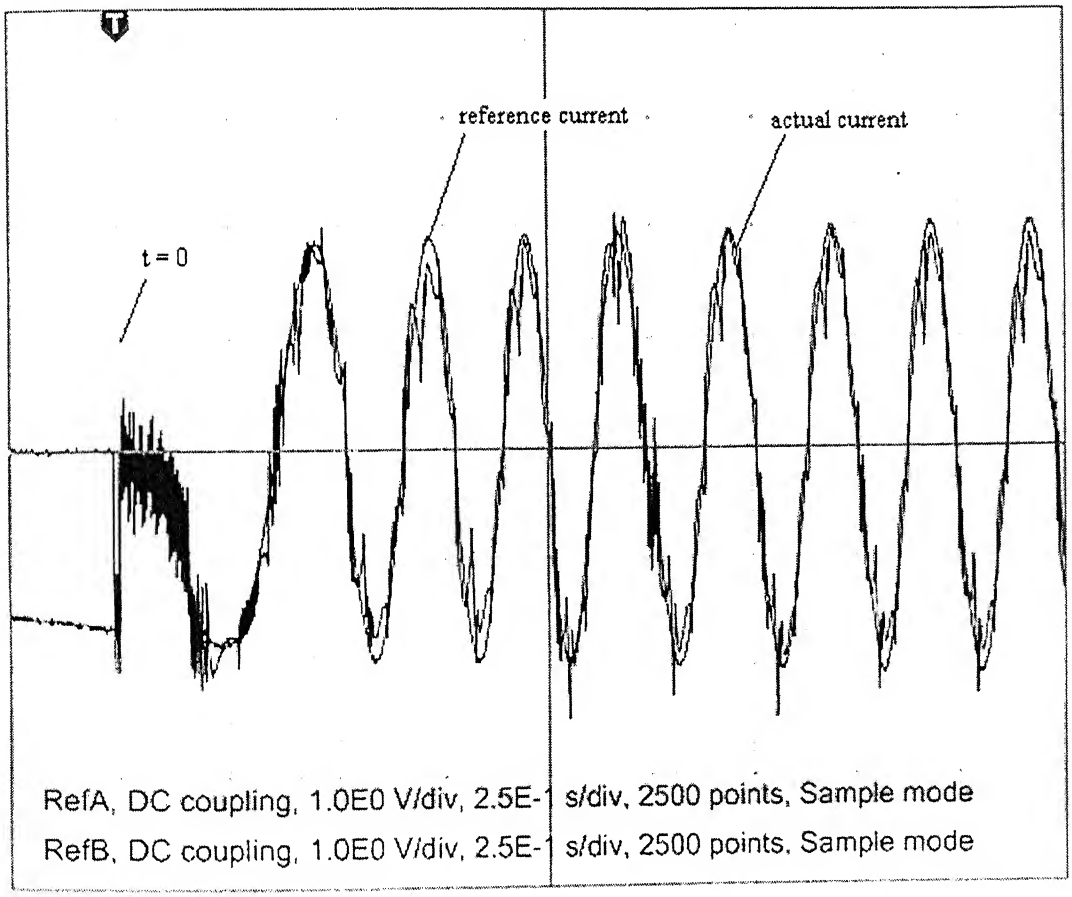

Fig. 3.12 (a) Reference and actual currents of phase – A during starting period.

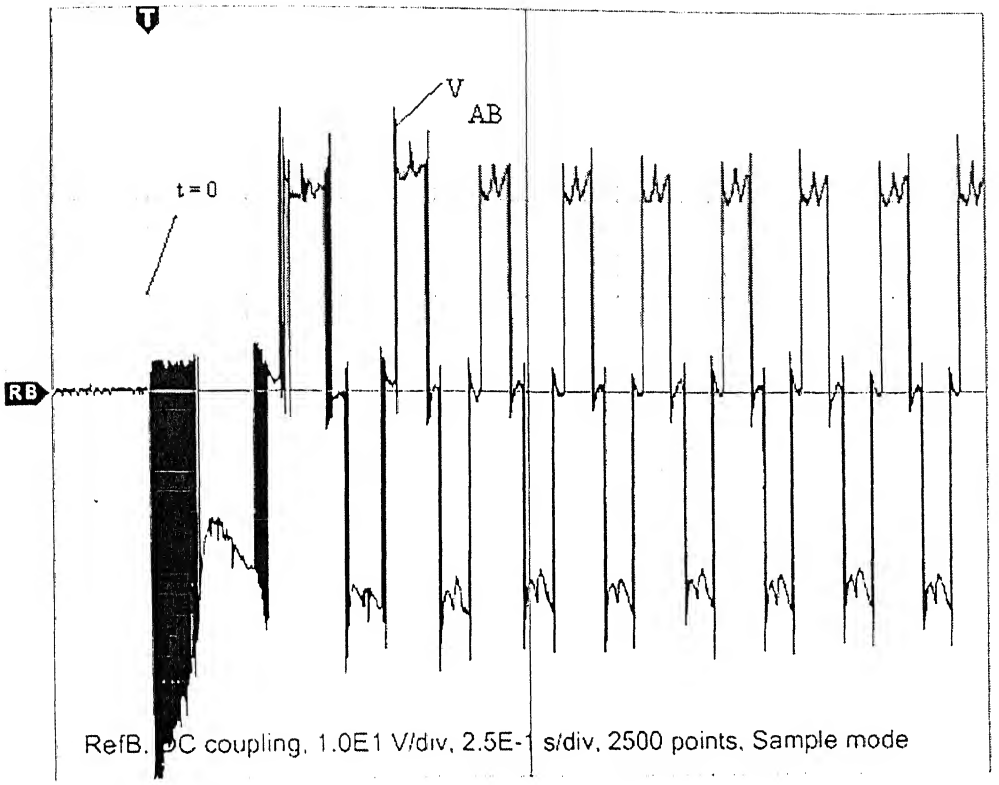

Fig. 3.12 (b) Line – Line voltage V_{AB} during starting period.

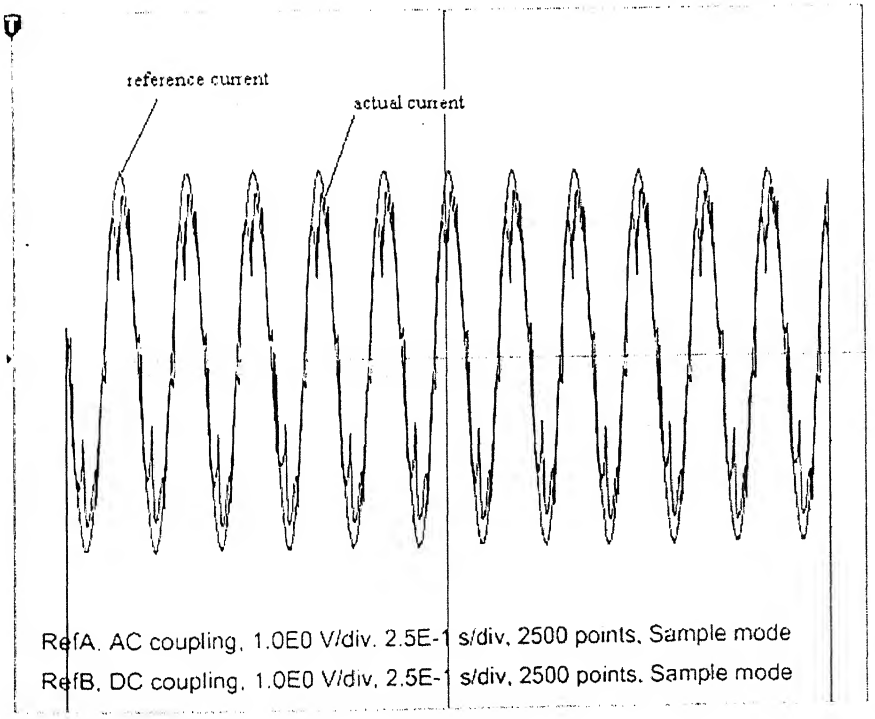

Fig. 3.13 (a) Steady state oscillogram of reference and actual currents of phase –A.

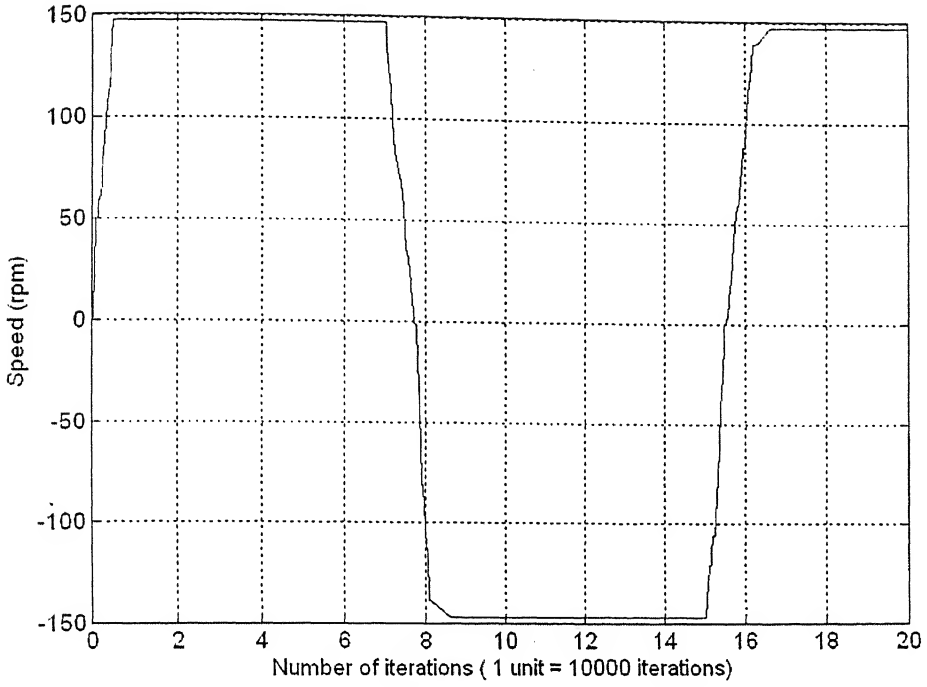

Fig. 3.14 Speed response for multiple speed reversals.

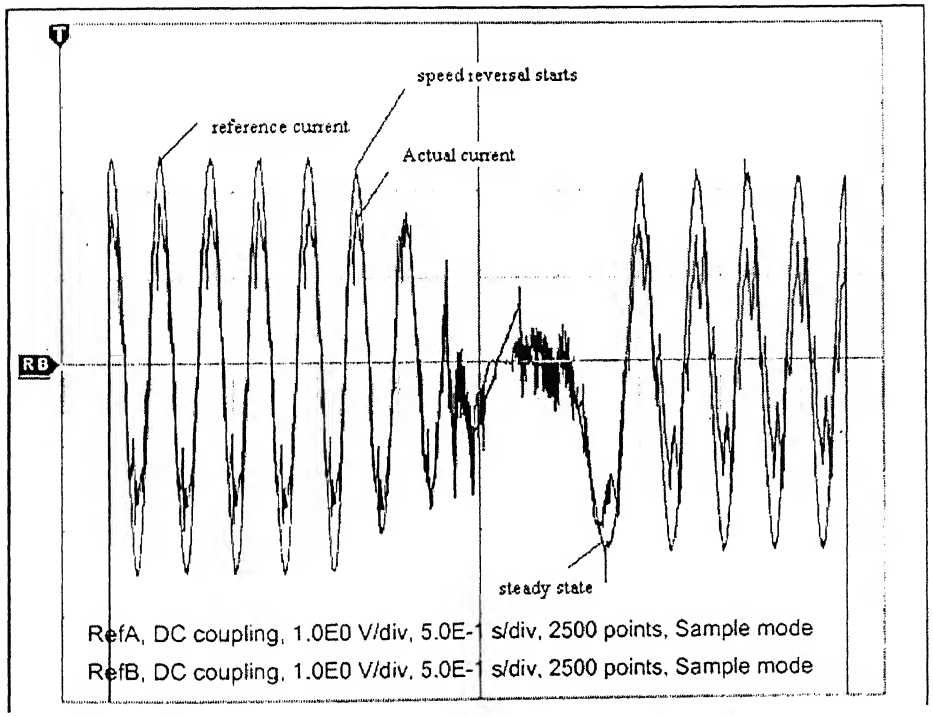

Fig. 3.15(a) Reference and Actual current of phase-A during speed reversal.

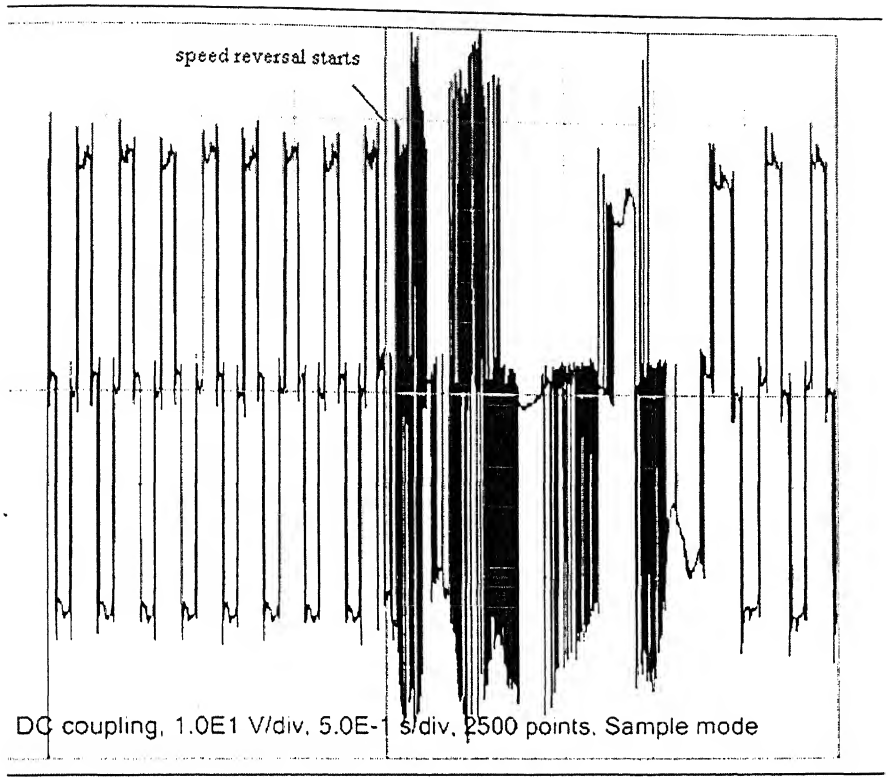

Fig. 3.15(b) Line –Line voltage V_{AB} during speed reversal.

3.9 Conclusion

The drive is operated in self–controlled mode where the field position information is used to excite the stator terminals of SM. Field orientation principle is used to decouple the d-axis from stator windings, which requires rotor position feedback and a constant field current. Drive was tested for speed command of 150 rpm and also for multiple speed reversals from +150 rpm to -150 rpm then again to +150 rpm. The behaviour of drive was found to be satisfactory.

Chapter 4

Conclusions and Scope for Future Work

4.1 Contributions of Present Thesis Work

Initially, the modeling and simulation of a Vector controlled SM drive with i_{ds}=0 is presented in the thesis. Digital models for synchronous motor, 3-phase inverter, hysteresis controller are developed. Simulation of drive for change in speed and torque, speed and torque reversals is done. Corresponding plots of various parameters are plotted. The dynamic response of drive is fast with vector control (constant field control).

Subsequently, the hardware implementation of a vector controlled SM drive with constant field control is discussed. Design and fabrication of 3-phase inverter, hysteresis controller and auxiliary circuits like current sensor, adder circuit are described. Algorithm used to control the drive is also outlined. The experimental CRPWM inverter fed SM drive is tested for different speed commands and multiple speed reversals. The response of practical drive system is found to be satisfactory.

The salient contributions of present thesis work can, thus, be summarized as follows:

1. Modeling and simulation a CRPWM inverter fed Vector controlled wound field synchronous motor drive for $i_{ds} = 0$ is carried out.
2. Practical implementation of a CRPWM inverter fed Vector controlled field synchronous motor drive with constant field current.

4.2 Applications of a Vector Controlled SM Drive

Vector controlled SM drives are widely used in both industrial and commercial motor applications. For the high power drives with power ratings from just below 1MW up to 10 MW and even 100 MW in special cases, wound field SM provides most plausible choice for motion control [21]. A number of applications are given in this section to illustrate the diversity of application.

1. In drives intended for traction applications or spindle drives for machine tools a very wide speed range including a constant power mode is required. A vector controlled, wound field SM is well suited to such requirements since it can be field weakened when operated below base speed [22].
2. High power drives using CSI power converters and wound field SM are used for fan and compressor drives.
3. SM motors driven by PWM current regulated inverters are used for ship propulsion [23]. In this case the control is field orientation and the machine is constructed as an eleven phase machine to reduce the size of individual converter legs. Each phase is driven by a separate PWM inverter arrangement which consists of small converters each feeding a separate portion of phase winding.

4.3 Scope for future work

There exists scope for further investigation /development on the existing drive system. They can be enumerated as follows

1. Simualtion and modeling of a Vector controlled SM drive with a non –zero value of i_{ds} can be carried out. The reference flux component of stator current is generated in such a manner that during transient period the response delay of

field current is nullified so as to assist in maintaining constant stator flux linkage (even in transient period). For this condition the drive will be operating in unity power factor.

2. PI controller is used in the speed loop, which has to be tuned for each different range of speeds. Also the PI controller is very much sensitive to system parameters. So to over come this problem, control techniques like sliding mode control can be used. A robust sliding mode control for a PM SM is described [24]. The control strategy is based on MIMO second order sliding mode approach. Under an assumption on the choice of controller gains, it is proved that the control law converges in spite of the parameters uncertainties and the outputs coupling.
3. In this developed drive system there is no feature of auto-start–up. For the drive system to become self-starting, the initial rotor position should be known. When the control circuit is powered on, the rotor alignment is arbitrary and the incremental encoder as it is does not provide correct position information. A novel method [16] has been developed to find out the initial position of rotor, thus making drive self starting.
4. Practical implementation of Vector Controlled SM drive with field excitation controller can be carried out.

REFERENCES

1. R. E. Doherty, C. A. Nickle, "Part I, An Extension of Blondel's two reaction theory", *Trans. AIEE*, pp. 912 , 1929 ; "Part II, Steady power angle characteristics", *Trans. AIEE*, pp. 927 ,1926.

2. R. H. Park, "Two Reaction theory of synchronous machine", Part I, *Trans. AIEE*, pp. 716, 1929.

3. F. Blaschke, "A new method for the structural decoupling of AC Induction machines," *IAFC Symposium*, Düsseldorf, Germany, pp. -15, Oct.1971.

4. K. H. Bayer, H. Waldmann and M. Weibelzahl, "Field orientated closed-loop control of a synchronous machine with NEW Transvektor control system," *Siemens Review*, Vol. 39, no. 5, pp. 220-223, 1972.

5. W. Leonhard, *Control of Electrical Drives*, Springer-Verlag, 1996.

6. P. Vas, *Vector Control of AC Machines*, Clarendon Press, 1990.

7. P. C. Krause, *Analysis of Electric Machinery, New* York: McGraw-Hill, 1987.

8. E. F. W. Alexanderson and A. H. Mittag, "The Thyratron motor," *Electrical Engg.*, Vol. 54, pp. 1517-*1523, 1934.*

9. T. Kataoka and S. Nishikata, "Transient performance analysis of self-controlled synchronous motors," *IEEE Transactions Industrial Applications*, Vol. IA-17, no. 2, pp. 152-59, March/April 1981.

10. H. Le-Huy, A. Jakubowicz, and R. Perret, "A self-controlled synchronous motor drive using terminal voltage system," *IEEE Transactions Industrial Applications*, Vol. IA-18, no. 1, pp. 46-53, Jan./Feb. 1982.

11. A. V. Gumaste and G. R. Slemon, "Steady-state analysis of a permanent magnet synchronous motor drive with voltage-source inverter," *IEEE Transactions Industrial Applications,* Vol. IA-17, no. 2, pp. 143-151, March/April 1981.

12. K. Zawirski, "Dynamic control of self-commutated synchronous motor in field constant and field weakening range," *in Conf. Pub.EPE (Brighton)*, pp. 332-337, 1993.

13. S. Fukuda, Y. Itoh, and A.Nii, "A microprocessor-controlled speed regulator for commutatorless motor drive," *Transactions IEE of Japan*, Vol. 104, no. 9/10, pp. 185-192, Sept./Oct. 1984.

14. L. J. Jacovides, M. F. Matouka, D.W.Shimer, "A cycloconverter-synchronous drive for traction applications," *IEEE Transactions Industrial Applications*, Vol. IA-17, no. 4, pp. 407-418, July/Aug. 1981.

15. P. S. Bimbhra, *Generalized theory of Electrical machines*, Chapter 4, pp. 195-203.

16. B. K. Bose, *Power Electronics and AC Drives,* Englewood Cliffs, NJ: Prentice-Hall, 1986.

17. Data sheet of M57959L Mitsubishi hybrid IC, Mitsubishi Electric Corporation.

18. R. A. Gayakwad, *Op-Amps and Linear Integrated Circuits, 3rd edition,* 1995, PHI New Delhi.

19. Y. Dote, *Servo Motor and Motion Control Using Digital Signal Processors.* Englewood Cliffs, NJ: Prentice Hall, 1990.

20. S. P. Das, "Design, Simulation and PC –based Implementation of a High Performance Cycloconverter –fed SM drive system," PhD. thesis, IIT Kharagpur, India, Sept.1996.

21. G. R. Slemon, "Electrical machines for variable –frequency drives," *Proc .IEEE,* Vol. 82, no. 8, pp. 1123- 1139, August 1994.

22. T. M. Jahns, G. B. Kliman and T. W. Neumann, "Interior permanent magnet synchronous motors for adjustable speed drives," *IEEE-IAS annual meeting conf record,* pp. 814-823, 1985.

23. H. Bausch, "Large power variable speed ac machines with permanent magnet excitation," *Proc Electric Energy Conf 1987,* Adelaide, pp. 265-271, Oct. 1987.

24. S. Laghrouche, F. Plestan and A. Glumineau, "Robust second order sliding mode control for a permanent magnet synchronous motor," *American Control Conference,* pp. 4071 -76, June *2003.*

APPENDIX A

Parameters of Machine

Stator – Field: 220 V max, 1.4 A max, DC, Salient pole.

Rotor – Armature: 3 –phase, star connected, 4-pole, 1500 rpm, 400V, 6A, 50 Hz.

$$\text{Turns ratio} = \frac{N_f(per\ pole)}{N_a(per\ \text{phase per pole})} = 15.$$

Parameters :

1. Armature resistance, $r_s = 2.73\ \Omega$.

2. Field resistance, $r_f = 1\ \Omega$.

3. Armature leakage inductance, $L_{la} = 0.0236$ H.

4. q-axis leakage inductance, $L_{ds} = 0.1186$ H.

5. q- Axis leakage inductance, $L_{qs} = 0.0939$ H.

6. Field leakage inductance, $L_{lf} = 0.005$ H.

7. Field self inductance, $L_f = 0.1$ H.

8. d-axis damper winding resistance, $r_{kd} = 6.609\ \Omega$.

9. q-axis damper winding resistance, $r_{kq} = 1.692\ \Omega$.

10. d-axis damper leakage inductance, $L_{lkd} = 0.0255$ H.

11. q-axis damper leakage inductance, $L_{lkq} = 0.04199$ H.

12. d-axis damper self inductance, $L_{kd} = 0.1205$ H.

13. q-axis damper self inductance, $L_{kq} = 0.11229$ H.

14. Moment of Inertia, $J = 0.0881$ Kg-m^2.

DC machine Parameters :

Armature: 220 V, 13.8 A, 3 kW, $r_a = 9.5\ \Omega$.

Field: Shunt, 220 V, 0.8 A.

APPENDIX B

Specifications of Components

This section gives details and specifications of IC's, IGBT, Data Acquisition card and Timer card and other accessories used in experiment.

B.1 IC 74123

Features

1. DC triggered from active-high transition or active-low transition inputs
2. Retriggerable to 100% duty cycle.
3. Direct reset terminates output pulse.
4. Compensated for VCC and temperature variations.
5. DTL, TTL compatible.
6. Input clamp diodes.

Functional Description

The basic output pulse width is determined by selection of an external resistor (RX) and capacitor (CX). Once triggered, the basic pulse width may be extended by retriggering the gated active-low transition or active-high transition inputs or be reduced by use of the active-low transition clear input.

The output pulse width (T_W) for $C_X > 1000$ pF is defined as follows:

$$T_W = K R_X C_X (1 \text{ a } 0.7/R_X)$$

where [R_X is in Kilo-ohm]

[C_X is in pico Farad]

[T_W is in nano second]

[$K \approx 0.28$]

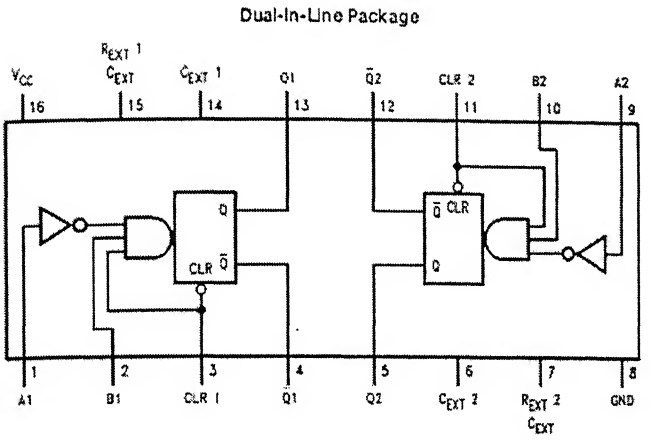

Triggering Truth Table

Inputs			Response
A	B	CLR	
X	X	L	No Trigger
↓	L	X	No Trigger
↓	H	H	Trigger
H	↑	X	No Trigger
L	↑	H	Trigger
L	H	↑	Trigger

H = HIGH Voltage Level
L = LOW Voltage Level
X = Immaterial

Fig. B.1 Pin diagram and Truth table of IC 74123.

B.2 TL084:

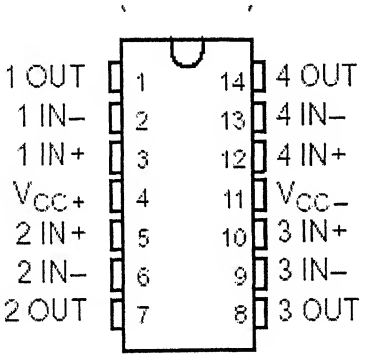

Fig. B.2 Pin diagram of TL084 (quad op-amp).

The TL084 JFET-input operational amplifier is designed to offer a wider selection than any previously developed operational amplifier family. This JFET-input operational amplifier incorporates well-matched, high-voltage JFET and bipolar transistors in a monolithic integrated circuit. The devices feature high slew rates, low input bias and offset currents, and low offset voltage temperature coefficient. Offset adjustment and external compensation options are available within the TL084.

B.3 Current sensor:

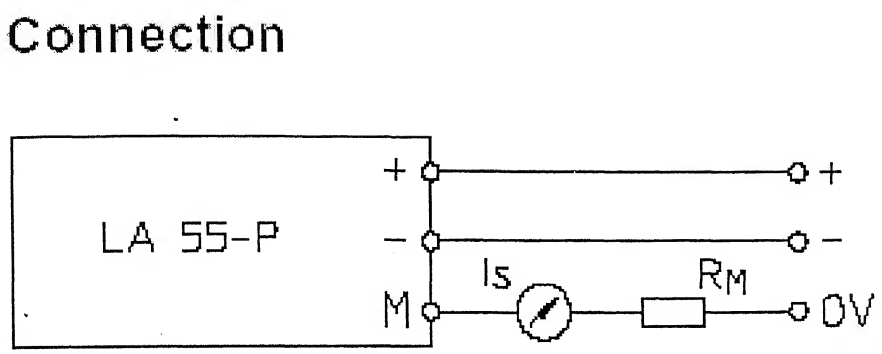

Fig. B.3 Pin diagram of current sensor LA 55-P.

Advantages:

Excellent accuracy.

Very good linearity.

Optimized response time.

Wide frequency bandwidth.

Current overload capability.

Features

Closed loop (compensated) current.

Transducer using the Hall Effect.

Insulated plastic case recognized.

Electrical data

Conversion ratio = 1:1000.

Measuring resistance =100Ω.

Supply voltage = ±12V.

Number of turns =7.

Secondary nominal r.m.s. current = 50 mA.

B.4 M57959L Mitsubishi Hybrid IC's for driving IGBT modules

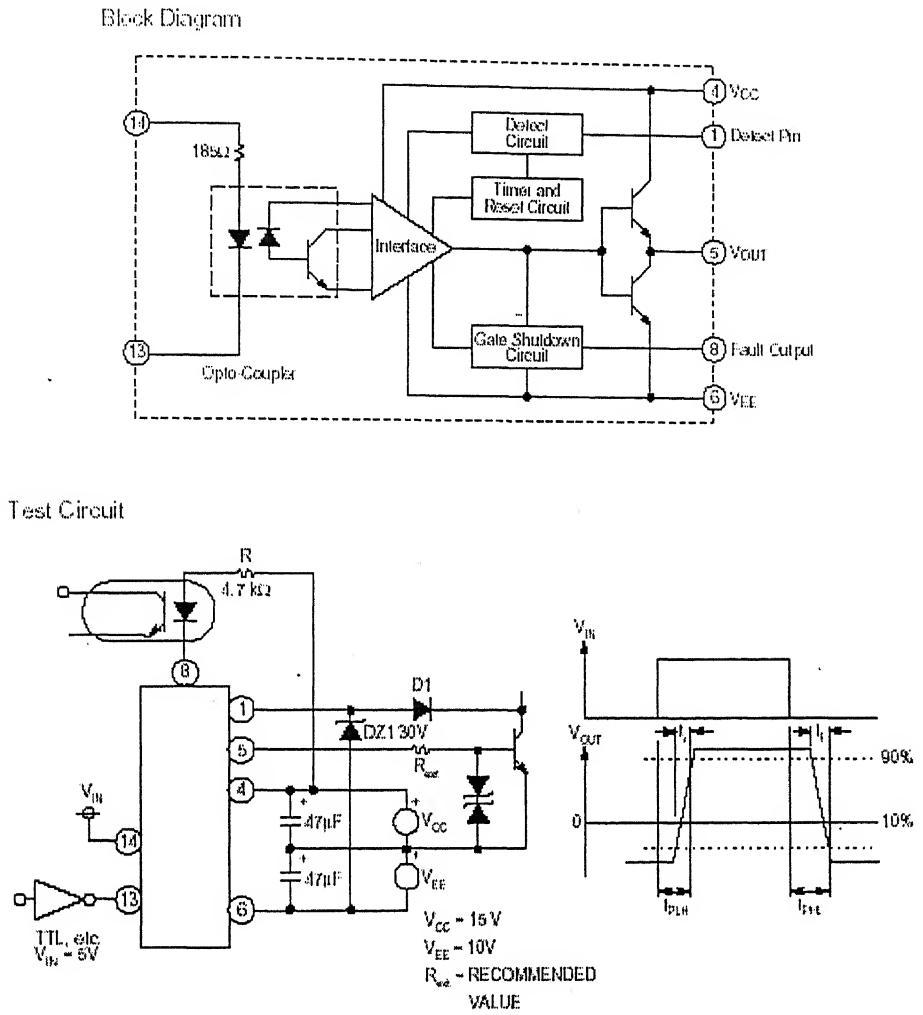

Fig. B.4 Block diagram and Test circuit of IGBT driver (M57959L).

Description:

M57959L is a hybrid integrated circuit designed for driving n-channel IGBT modules in any gate amplifier application. This device operates as an isolation amplifier for these modules and provides the required electrical isolation between the input and output with an opto-coupler. Short circuit protection is provided by a built in desaturation detector. A fault signal is provided if the short circuit protection is activated.

Features:

1. Built in high CMRR optocoupler (V_{CMR} : Typical30kV/ms, Min. 15kV/ms).

2. Electrical Isolation between input and output with opto-couplers.

3. Built in short circuit protection circuit with a pin for fault output.

Electrical Characteristics:

Supply voltage : V_{CC} = +15 V.

V_{EE} = -9V (20V ≤ V_{CC}+V_{EE} ≤ 28V).

Input voltage : V_{IN} = 1 to 7V (~).

Output Current: I_{OHP} -2 Amperes (Pulse Width 2ms, f = 20 kHz).

I_{OLP} 2 Amperes (Pulse Width 2ms, f = 20 kHz).

Output Voltage: V_{OH} = +14 Volts.

V_{OL} = -8 Volts.

Time constants:

L-H Propagation Time	t_{PLH}	1.5 μs.
L-H Rise Time	t_r	1.0 μs.
H-L Propagation Time	t_{PHL}	1.5 μs.
H-L Rise Time	tr	0.6 μs.

Application: To drive IGBT modules for inverter, AC Servo systems, UPS, CVCF inverter, and welding applications.

B.5 CM50DU-24F Mitsubishi IGBT modules

CM50DU-24F

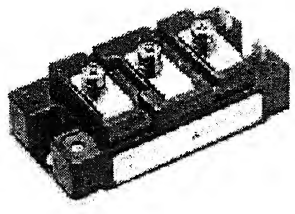

- IC 50A
- VCES 1200V
- Insulated Type
- 2-elements in a pack

Circuit Diagram:

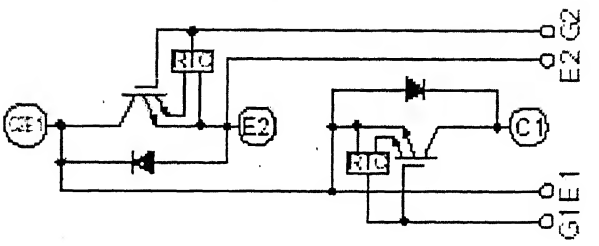

Fig. B.5 IGBT Module circuit diagram.

MAXIMUM RATINGS (T_j = 25°C)

Symbol	Parameter	Conditions	Ratings	Unit
V_{CES}	Collector-emitter voltage	G-E Short	1200	V
V_{GES}	Gate-emitter voltage	C-E Short	±20	V
I_C	Collector current	T_c = 25°C	50	A
I_{CM}		Pulse (Note 2)	100	A
I_E (Note 1)	Emitter current	T_c = 25°C	50	A
I_{EM} (Note 1)		Pulse (Note 2)	100	A
P_C (Note 3)	Maximum collector dissipation	T_c = 25°C	320	W
T_j	Junction temperature		−40 ~ +150	°C
T_{stg}	Storage temperature		−40 ~ +125	°C
V_{iso}	Isolation voltage	Charged part to base plate, AC 1 min.	2500	V
—	Torque strength	Main Terminal M5	2.5 ~ 3.5	N • m
		Mounting holes M6	3.5 ~ 4.5	N • m
—	Weight	Typical value	310	g

ELECTRICAL CHARACTERISTICS (T_j = 25°C)

Symbol	Parameter	Test conditions	Limits			Unit
			Min.	Typ.	Max.	
I_{CES}	Collector cutoff current	V_{CE} = V_{CES}, V_{GE} = 0V	—	—	1	mA
$V_{GE(th)}$	Gate-emitter threshold voltage	I_C = 5.0mA, V_{CE} = 10V	5	6	7	V
I_{GES}	Gate leakage current	V_{GE} = V_{CES}, V_{CE} = 0V	—	—	20	uA
$V_{CE(sat)}$	Collector-emitter saturation voltage	T_j = 25°C, I_C = 50A, V_{GE} = 15V	—	1.8	2.4	V
		T_j = 125°C, I_C = 50A, V_{GE} = 15V	—	1.9	—	
C_{ies}	Input capacitance	V_{CE} = 10V, V_{GE} = 0V	—	—	20	nF
C_{oes}	Output capacitance		—	—	0.85	nF
C_{res}	Reverse transfer capacitance		—	—	0.5	nF
Q_G	Total gate charge	V_{CC} = 600V, I_C = 50A, V_{GE} = 15V	—	550	—	nC
$t_{d(on)}$	Turn-on delay time	V_{CC} = 600V, I_C = 50A, V_{GE1} = V_{GE2} = 15V, R_G = 6.2Ω, Inductive load switching operation, I_E = 50A	—	—	100	ns
t_r	Turn-on rise time		—	—	50	ns
$t_{d(off)}$	Turn-off delay time		—	—	300	ns
t_f	Turn-off fall time		—	—	300	ns
t_{rr} (Note 1)	Reverse recovery time		—	—	150	ns
Q_{rr} (Note 1)	Reverse recovery charge		—	2.1	—	uC
V_{EC} (Note 1)	Emitter-collector voltage	I_E = 50A, V_{GE} = 0V	—	—	3.2	V
$R_{th(j-c)Q}$	Thermal resistance*1	IGBT part (1/2 module)	—	—	0.39	°C/W
$R_{th(j-c)R}$		FWDi part (1/2 module)	—	—	0.70	°C/W
$R_{th(c-f)}$	Contact thermal resistance	Case to fin, Thermal compound applied*2 (1/2 module)	—	0.07	—	°C/W
$R_{th(j-c')Q}$	Thermal resistance	Tc measured point is just under the chips.	—	—	0.31*3	°C/W
R_G	External gate resistance		6.3	—	63	Ω

Note 1. If V_{EC}, t_{rr}, Q_{rr} doesn't represent characteristics of the anti-parallel, emitter to collector free-wheel diode (FWDi).
2. Pulse width and repetition rate should be such that the device junction temp. (T_j) does not exceed T_{jmax} rating.
3. Junction temperature (T_j) should not increase beyond 150°C.

*1 : Tc measured point is indicated in OUTLINE DRAWING.
*2 : Typical value is measured by using Shin-etsu Silicone "G-746".
*3 : If you use this value, $R_{th(f-a)}$ should be measured just under the chips.

B.6 ACL-8112 PG Enhanced Multi-function Data Acquisition Cards

Introduction

The ACL-8112 PG Series is a high speed analog and digital I/O card for PC/AT compatible computers. This card is the new generation of industrial standards ACL-812PG and PCL-812PG from AD Link.

Features

1. 12-bit analog input resolution.
2. Up to 100k Hz A/D sampling rate.
3. ACL-8112PG is 16 single-ended channels.
4. ACL-8112PG is bipolar input.
5. Programmable gain selection.
6. On-chip sample & hold.
7. Two 12-bit monolithic multiplying analog output channels.
8. 16 digital input/output channels.
9. 3 independent programmable 16-bit down counters.
10. Three A/D trigger modes: software trigger, programmable pacer trigger, and external pulse trigger.
11. Integral DC-to-DC converter for stable analog power source
12. AT bus with 9 IRQ levels

Specifications:

Analog Input (A/D)

1. Converter: B.B. ADS774 or equivalent.
2. Resolution: 12 bits.
3. Converter type: successive approximation.

4. Number of input channels: 16 single-ended (ACL-8112PG).

5. Analog input range: (programmable)

   Bipolar: ±10V, ±5V, ±2.5V, ±1.25V, ±0.625V, ±0.3125V.

6. Over-voltage protection: Continuous ±35V maximum.

7. Accuracy

GAIN = 1	0.01% of FSR ±1 LSB
GAIN = 2, 4	0.02% of FSR ±1 LSB
GAIN = 8, 16	0.04% of FSR ±1 LSB

9. Input impedance: 10 MΩ

10. Trigger mode: Software, Pacer, and External trigger.

11. Data transfer: Program control, interrupt, DMA.

12. Sampling rate: 100 KHz maximum for single channel by DMA data transfer.

Analog Output (D/A)

1. Numbers of channel: 2 double-buffered analog outputs.

2. Resolution: 12-bit.

3. Output range

   • Internal reference:

   (Unipolar) 0~5V or 0~10V.

   • External reference:

   (Unipolar) max. +10V or -10V.

4. Converter: B.B 7541 or equivalent, monolithic multiplying.

5. Settling time: 30 μ sec.

6. Linearity: ±1/2 bit LSB.

7. Output driving capability: ±5mA max.

Digital I/O (DIO)

1. Number of channels: 16 TTL compatible inputs and 16 TTL compatible outputs.

2. Input voltage

   • Low: Min. 0V; Max. 0.8V.

   • High: Min. +2.0V.

3. Input load

   • Low: +0.5V@0.2mA max.

   • High: +2.7V@+20mA max.

4. Output voltage

   • Low: Min. 0V; Max. 0.4V.

   • High: Min. +2.4V.

5. Driving capacity

   • Low: Max. +0.5V at 8.0mA (Sink).

   • High: Min. 2.7V at 0.4mA (Source).

Programmable Counter

- Device: 8254 or equivalent.
- A/D pacer: 32-bit timer (two 16-bit counters cascaded) with 2 MHz time base.
- Pacer frequency range: 0.00046 Hz ~ 100 kHz.
- Counter: One 16-bit counter with a 2 MHz time base.

General Specifications

- I/O base address: 16 consecutive address locations.
- Connector: 37-pin D-type connector.
- IRQ level: (9 levels jumper selectable) 3, 5, 6, 7, 9, 10, 11, 12, 15.

- DMA: CH1 or CH3 (jumper selectable).
- Operating temperature: 0° ~ 55°C.
- Storage temperature: -20° ~ 80°C.
- Power requirement
  - +5V @ 450 mA typical.
  - +12V @ 150 mA typical.

Default Base Address: 300 HEX.

B.7 PCL-223: Multifunction Timer / Counter card

PCL-223 is a multifunction timer/counter card with 9 channels of 16 bit timers/counters using three 8253 chips. One of these chips is provided with cascading facility for all three channels, as well as interrupt generation facility. Second 8253 is provided with optoisolated input/output and the third 8253 is directly available for external connection through a FRC connector. In addition to the timer/counter PCL-223 has 8 TTL input lines and 8 TTL output lines.

Applications:

- Programmable baud rate generation.
- SCR firing angle control.
- Frequency synthesizer, frequency shift keying.
- Triggerable digital timing applications.
- Coincidence alarm.

Features

Timer/Counter

1. Three channels with optoisolated Gate, Clock and Output signals, three channels with cascading and interrupt generation facility, three totally user configurable channels.
2. Input frequency: for nonisolated channels: DC to 2.4MHz.

   for isolated channels: DC to 5 kHz.
3. On-board clock generator with programmable divider.

Digital I/O

8 TTL input lines, 8 TTL output lines.

B.8 Voltage Regulators: Two types of voltage regulators are used. Positive fixed voltage regulators like 7805 (+5V), 7812 (+12V), 7815 (+15V) and negative fixed voltage regulator like 7909 (-9V) and 7912 (-12V).They can deliver output current up to 1A. They also have thermal overload and short circuit protection.

Internal Block Digram

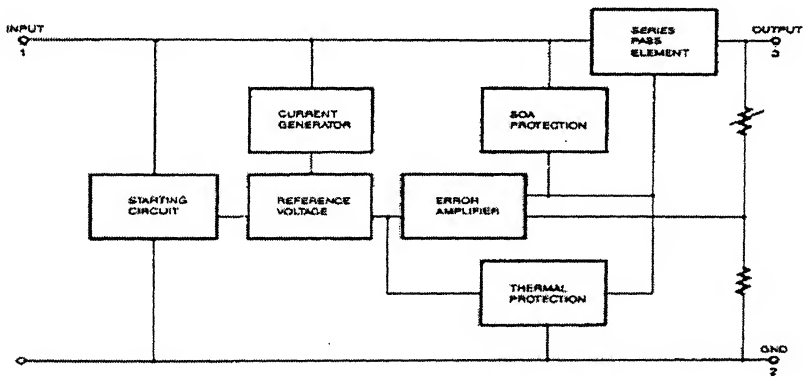

Fig. B.6 Internal Block diagram of Voltage regulator.

Positive voltage regulators:

1. Input 2.GND 3.output

Negative voltage regulator:

1. GND 2.Input 3.Output (for negative voltage regulators Input should be negative voltage)

APPENDIX C

Listing of PC Interface Program

```
/* Real time Program for Vector Control of SM (with constant If) */
/* counter A0, C0, C1 are used for time, speed and theta respectively*/

#include<stdio.h>

#include<conio.h>

#include<time.h>

#include<math.h>

#include<dos.h>

#define Base 0x200

#define BaseAddress 0x300

main ()
{

unsigned finaltheta, i=0, s;

unsigned readm =0, readl=0, initialvalue, finalvalue;

unsigned initialtime, finaltime, dn, readl1, readl2, readm1, readm2;

unsigned lsb1,msb1,lsb2,msb2,tlsb2,tmsb2,count,thetadiff;

unsigned time, pulsecount, signN=1, signO=1,dirP=0,dirN=0,val,dir;

float wref=0.0, speed=0.0,theta=0.0,wri=0.0,wrj,sf=0.024,TH0=0.0,t=0.0;

                        //wr(i)= wri, wr(i+1) = wrj,sf = 60/2500;

float Ai=0.0,Aj,kp=.01,ki=.001,Bi=0.0,Bj=0.0,h=0.0013,ias,ibs,Bx=0.0;

float CNT0=0.0;

FILE *fpt;

clrscr();

fpt = fopen ("speed.dat","w");

outportb(Base+12,0x03); // internal frequency is 250 kHz

outportb(Base+16,0x41); //gates of A0 and C0 are software triggered

outportb(Base+3,0x30); //select counterA0,write lsb & then msb in mode0

outportb(Base+0,0xff); // lsb of counter A0 is initialised to ff

outportb(Base+0,0xff); // lsb of counter A0 is initialised to ff
```

```
outportb(Base+11,0x30);//select counterC0 write lsb & then msb in mode0
outportb(Base+8,0xff); // lsb of counter C0 is initialized to ff
outportb(Base+8,0xff); // msb of counter C0 is initialized to ff
outportb(Base+11,0x72);//select counterC1 write lsb & then msb in mode1
outportb(Base+9,0xff); // lsb of counter is initialised to ff
outportb(Base+9,0xff); // msb of counter is initialised to ff
s=0xFFFF-0x4350;
while (t < 30.0)          // main loop starts
      {
      if (t >7.0 && t < 15.0)      // speed reversal from +150 to -150
      wref = -150.0;
      if (t > 15.0)                // speed reversal from -150 to +150
      wref = 150.0;
      /* theta calculation starts */
      outportb(Base+11,0x42);
      readl=inportb(Base+9);
      readm=inportb(Base+9);
      count=readm * 0x100 + readl;
      thetadiff = (0xffff-count);
      Bx = thetadiff * 0.005026;
      /* checking direction */
      val=inportb(BaseAddress+6);
      if (val == 255)
      signN=1;       // signN = 1 implies forward direction
      else
      signN=0;       // signN = 0 implies reverse direction
      dir = 10 * signN + 1 * signO;
     if(signN != signO)//if direction is changed do the following
```

```
{
 CNT0 = Bx;
 TH0 = theta;
 dirN = 0;
 dirP = 0;
 }
/* direction checking is over */
 if ((dir==11) && (dirP==0))     //forward direction
 {
 theta = Bx;
 if (theta > 12.56637)
 theta =theta-12.56637;
 }
 if ((dir==00) && (dirN==0))     //reverse direction
 {
 theta = 12.56637 - Bx;
 if (theta < 0)
 theta = theta+12.56637;
 }
 if (dir==10|| dirP==1)       //reverse to forward, signN=1,signO=0
 {
    if (CNT0 > Bx)              //if marker pulse comes make dirP=0
      dirP=0;                     // otherwise calculate theta
    else if (CNT0 <= Bx)
    {
    theta = TH0 + Bx - CNT0;
    dirP=1;
    }
 }
```

```
if (dir==1 || dirN==1)        //forward to reverse ,signN=0,signO=1
{
   if (CNT0 > Bx)             //if marker pulse arrives make dirN=0
      dirN=0;                  //otherwise calculate theta
    else
      {
      theta = TH0 +CNT0 -Bx;
      dirN=1;
      }
    if (theta < 0)
    theta = theta+12.556637;
}
signO = signN;
/* theta calculation is completed */
/* speed calculation starts */
outportb(Base+11,0x00); //select counterC0,mode0 & counter latch
readl1 = inportb(Base+8);      //read lsb of C0 (speed counter)
readm1 = inportb(Base+8);      //read msb of C0 (speed counter)
initialvalue=readm1*0x100+readl1; //initial value of C0 is read
outportb(Base+3,0x00);         // counterA0,mode0 & count latch
tlsb2 = inportb(Base+0);       // read lsb of A0 (time counter)
tmsb2 = inportb(Base+0);       // read msb of counter A0
finaltime = tmsb2*0x100+lsb2; //final value of A0 is calculated
outportb(Base+11,0x00);        // counterC0,mode0 & counter latch
readl2 = inportb(Base+8);      // read lsb of C0 (speed counter)
readm2 = inportb(Base+8);      // read msb of C0 (speed counter)
finalvalue=readm2*0x100+readl2; //final value of C0 is calculated
if (finaltime < s)
```

```
{
time=0xffff-finaltime;
pulsecount = 0xffff - finalvalue;
speed = pulsecount * sf/time;
speed = speed * pow10(6)/4;
outportb(Base+3,0x30);  //counterA0,write lsb & then msb in mode0
outportb(Base+0,0xff);  //lsb of counter A0 is initialised to ff
outportb(Base+0,0xff);  //lsb of counter A0 is initialised to ff
outportb(Base+11,0x30); //counterC0,write lsb & then msb in mode0
outportb(Base+8,0xff);  //lsb of counter C0 is initialised to ff
outportb(Base+8,0xff);  // msb of counter C0 is initialised to ff
}
/* speed calculation is completed */
/* PI controller starts */
wrj=speed;
if (t > 7.0 && t < 15.0)
  wrj = -1*speed;          // when wref is -150 then wrj = -speed
Bi=wref-wri;               //B(i)    = wref - wr(i)
Bj=wref-wrj;               //B(i+1)   = wref - wr(i+1)
Aj=Ai+kp*(Bj-Bi)+ki*Bj*h
wri=wrj;                    // now wr(i) = wr(i+1)
     /* limiter starts */
if (Aj >=3.5)
  Aj=3.5;
if (Aj<=-3.5)
  Aj=-3.5;
Ai=Aj;
     /* limiter ends */
```

```
    ias =0.692 * Aj * cos(theta+1.5707);
    ibs =0.692 * Aj * cos(theta-0.5237);
       //Aj = I_QS, while 0.69 is scaling factor for current sensor.
       /* PI controller is completed */
       /* digital to analog conversion of ias and ibs signals */
    dn = (ias*4096/5)+2047;//finding digital number equivalent of ias
    lsb1= dn & 0x00ff;        // generating lsb from digital number
    msb1= dn >> 8;            //to find msb, shift dn 8 places right
    msb1= msb1 & 0x000f;      //then AND the resultant number with 000f
    outportb(BaseAddress+4, lsb1); //write the lsb at BaseAddress+4
    outportb(BaseAddress+5,msb1);  //write the msb at BaseAddress + 5
    dn =(ibs*4096/5)+2047; //finding digital number equivalent of ibs
    lsb2 = dn & 0x00ff;     //generating lsb from digital number
    msb2 = dn >> 8;         //to find msb, shift dn 8 places right
    msb2 = msb2 & 0x000f;  //then AND the resultant number with 000f
    outportb(BaseAddress+6, lsb2);  //write the lsb at BaseAddress+6
    outportb(BaseAddress+7, msb2); //write the lsb at BaseAddress+7
    t=t+0.00001;
    if(i > 100)    // once in 100 iterations speed is written into
          {
           fprintf(fpt,"\n %f ",wrj);
           i=0;
           }
      i= i+1;
   }                                  // main loop ends
  fclose(fpt);                        // file is closed
}                                     // main program ends
```